

The **IT** University
of Copenhagen

On Data Structures from Symmetry Sets of 2D Shapes

Arjan Kuijper

Copyright © 2004, Arjan Kuijper

**IT University of Copenhagen
All rights reserved.**

**Reproduction of all or part of this work
is permitted for educational or research use
on condition that this copyright notice is
included in any copy.**

ISSN 1600-6100

ISBN87-7949-069-7

Copies may be obtained by contacting:

**IT University of Copenhagen
Rued Langgaards Vej 7
DK-2300 Copenhagen S
Denmark**

Telephone: +45 72 18 50 00

Telefax: +45 72 18 50 01

Web www.itu.dk

Preface and Summary

This technical report consists of 4 chapters that elaborate on technical report nr. 36, and focus on 2+1D Symmetry Sets: 2D Symmetry Sets in either a one-parameter family of perturbations, or radius space, or a multi-scale context. These chapters are included in article format, since they are all either published, or submitted, or intended to be submitted to conferences. Therefore, some overlap in text and / or figures occurs.

They are inspired by the results of the research written down in the deliverable 10. One part of this deliverable was presented at ECCV 2004 (focussing on the data structure induced by the Symmetry Set) [28], while a second part was presented at S+SSPR 2004 (concerning alternative representations of Symmetry Set, e.g. the pre-Symmetry Set) [26].

- Chapter 1 focusses on the changes that can occur in the Pre-Symmetry Set. They follow directly from possible changes of the Symmetry Set. It allows descriptions by means of a dynamic 2+1D Symmetry Set. This chapter has been presented at ICPR 2004 [27] and is the result of close collaboration with Ole Fogh Olsen (ITU) and Peter Giblin (Liverpool).
- Chapter 2 describes a possible application of the usage of the transitions, viz. amending the pre-Symmetry Set. It is a way to remove small details in the (pre-)Symmetry Set. This chapter is the result of collaboration with Ole Fogh Olsen (ITU).
- Chapter 3 describes a fast and elegant extraction of the Medial Axis once the (pre-)Symmetry Set is known. It uses the radius space as described in deliverable 10. This chapter is the result of collaboration with Ole Fogh Olsen (ITU).
- Chapter 4 describes a general multi-scale frame work, where the pre-Symmetry Set is embedded in a mean curvature motion structure - the intrinsic heat equation for shapes. It yields a hierarchical structure suitable for describing and comparing shapes. It is the result of collaboration with Ole Fogh Olsen (ITU), Peter Giblin (Liverpool), and Dirk Siersma (Mathematics, Utrecht).

Contents

1	Transitions of the Pre-Symmetry Set	7
1.1	Introduction	7
1.2	Symmetry Set	7
1.2.1	Points on the Symmetry Set	8
1.2.2	Transitions	8
1.3	Pre-Symmetry Set	9
1.3.1	Points on the Pre-Symmetry Set	9
1.4	Transitions of the pre-symmetry set	10
1.4.1	Curves on the diagonal: A_4	10
1.4.2	Curves of the diagonal: A_2^2 moth	10
1.4.3	Smoothing curves: A_1A_3	12
1.4.4	Swapping of branches: A_2^2 nib	12
1.4.5	Collision of four A_1^3 – points: A_1^4	12
1.4.6	(Dis)appearance of two A_1^3 – points: $A_1^2A_2$	13
1.5	Summary and Conclusions	13
2	Amending the pre-Symmetry Set	15
2.1	Introduction	15
2.2	Symmetry Set	15
2.2.1	Points on the Symmetry Set	16
2.2.2	Transitions	17
2.3	Pre-Symmetry Set	18
2.3.1	Points on the Pre-Symmetry Set	19
2.3.2	Transitions	19
2.4	Amending the pre-ss	20
2.4.1	Smoothing the pre-ss branches	20
2.4.2	Selecting pre-ss branches	22
2.5	Summary and Conclusions	22
3	Geometric Skeletonization	29
3.1	Introduction	29
3.2	Background	29
3.2.1	Medial Axis and Symmetry Set	29
3.2.2	Points on the Symmetry Set	30
3.2.3	pre-Symmetry Set	30
3.2.4	Points on the Pre-Symmetry Set	31
3.2.5	regularisation	31
3.3	Using the pre-ss	33
3.3.1	Branch types	33
3.3.2	Algorithm	34
3.4	Example	34
3.5	Summary and Conclusions	37

4	The Structure of Shapes	39
4.1	introduction	39
4.2	Background	40
4.2.1	Shapes	40
4.2.2	Evolution	40
4.2.3	Symmetry Set	41
4.2.4	pre-Symmetry Set	41
4.3	Representation	42
4.3.1	Properties of the pre-Symmetry Set	42
4.3.2	Gauss diagram	43
4.4	Multi-scale shape hierarchy	43
4.4.1	Comparison with Curvature Scale Space	44
4.4.2	Gauss Diagrams under Mean Curvature Motion	44
4.5	Conclusions	47

Chapter 1

Transitions of the Pre-Symmetry Set

Abstract

The Symmetry Set (\mathcal{SS}) and its subset the Medial Axis (\mathcal{MA}), can be used to describe a shape. The representation of the \mathcal{SS} in parameter space is called the pre-Symmetry Set. Changes in the shape are directly related to so-called transitions (topological changes) of the \mathcal{SS} . They have also effect on the Pre- \mathcal{SS} . Since the Pre- \mathcal{SS} can be used to represent the shape efficiently, it is important to study the transitions of the pre- \mathcal{SS} and their impact. We present these transitions, as well as the presence of the \mathcal{MA} in the pre- \mathcal{SS} .

1.1 Introduction

In shape analysis, much effort has been put into the research on the skeleton, or Medial Axis (\mathcal{MA}) [2], as a way to represent the shape in a more simplified way. As it was soon realized, the \mathcal{MA} it itself didn't carry enough information and sophisticated extensions were built. Next, the potential changes (transitions) of the \mathcal{MA} were investigated [15]. In that way different shapes can be related to each other for shape indexing and retrieval [35, 39]. The results on transitions boiled down from the results on the possible transitions [3] of the Symmetry Set (\mathcal{SS}) [4]. This set contains the \mathcal{MA} as subset. The \mathcal{SS} has its advantage in being easily described in mathematical sense, but its visualization is less pleasant for the eye. So most of the research has been focused on the (augmented) \mathcal{MA} .

Recently, however, a data structure was presented for the \mathcal{SS} [28], that can be visualized by a sequence of nodes, that are pair wise joined. This structure is related to the arc-annotated sequence used in RNA research [1]. Its main advantage over the graph structure used for the \mathcal{MA} is that it allows operations on it with a lower complexity.

In this paper we present a way to visualize the \mathcal{SS} in a more pleasing manner, by using the pre- \mathcal{SS} . Here we use pairs of points on the shape that give rise to a \mathcal{SS} point. So this avoids precise calculation of the \mathcal{SS} points in the plane. We present the possible transitions of the pre- \mathcal{SS} and discuss the relation of it to both the shape and its \mathcal{SS} . This opens ways to manipulate both by editing the pre- \mathcal{SS} , as presented in [28].

1.2 Symmetry Set

The Symmetry Set is defined as the closure of the loci of the circles tangent to a shape [4, 15]. In Figure 1.1a, the shape is given by the oval. Inside a circle is tangent to it at two locations, so the *unit* normals \mathcal{N}_1 and \mathcal{N}_2 are equal for the shape and the circle. The centre of the circle is found by multiplying minus the radius r with the normals. Note that this is also a \mathcal{MA} point. Next, also outside a circle is tangent to the shape at two locations, where the unit normals \mathcal{N}_3 and \mathcal{N}_4 are equal for the shape and the circle.

From this image it follows immediately that a point on the shape relates to at least two points on the \mathcal{SS} , in contrast with the \mathcal{MA} . A recipe for finding the \mathcal{SS} is the given by the following observations.

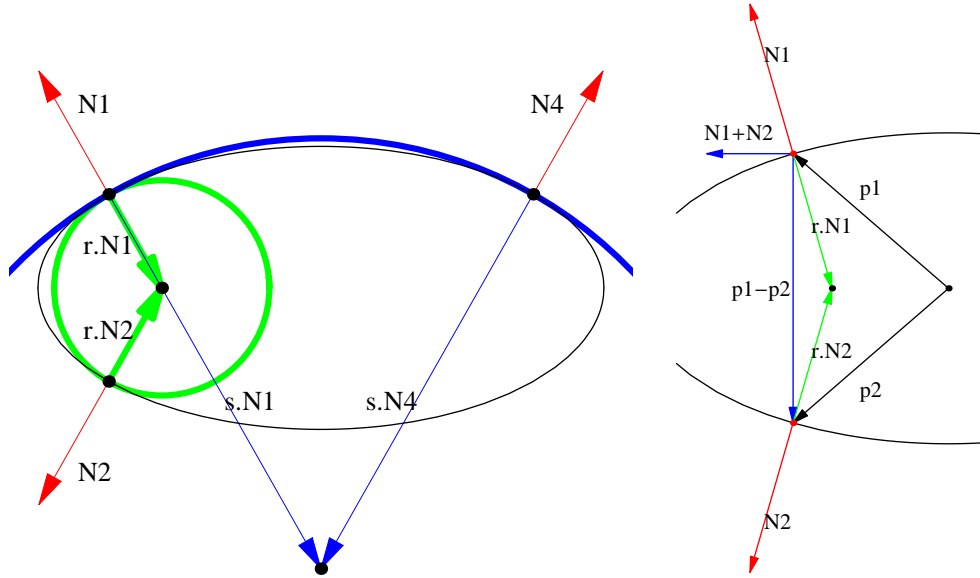


Figure 1.1: a) Circles tangent to a shape b) Computing the Symmetry Set (see text).

Let a circle be tangent to the shape as in Figure 1.1b. Then call the points at which it is tangent p_1 and p_2 . Then the vector $p_1 - p_2$ is perpendicular to the vector $\mathcal{N}_1 + \mathcal{N}_2$ when the circle is tangent twice from the same side as shown in these images, or to the vector $\mathcal{N}_1 - \mathcal{N}_2$, when tangent from two different sides (see [15]). So to find these locations it suffices to have a point p_i fixed and try all other points p_j along the shape and find zero crossings of $(p_i - p_j) \cdot (\mathcal{N}_i \pm \mathcal{N}_j)$. Next, the centre of the circle - the location of the \mathcal{SS} point - is given by $p_i - r\mathcal{N}_i = p_j \pm r\mathcal{N}_j$

Another tool that is used in the analysis of the \mathcal{SS} is the evolute. Let $\kappa(t) = (x_t y_{tt} - y_t x_{tt}) / (x_t^2 + y_t^2)^{-3/2}$ be the curvature of the shape \mathcal{S} , then the evolute is given by $\mathcal{S} + \mathcal{N} / \kappa$. In Figure 1.2a a shape, its evolute (thick line connecting endpoints in cusps) and the \mathcal{SS} (both lines) are shown. Its \mathcal{MA} is the vertical curve.

1.2.1 Points on the Symmetry Set

Due to the geometry of the shape and the order of tangency, four distinct types of points generically occur on the full \mathcal{SS} [4, 15].

A_1^2 points: the midpoints of circles tangent at two distinct points of the shape. These points are dense on the \mathcal{SS} .

An A_3 point: the midpoint of a circle located at the evolute and tangent at the point of the shape with the local extremal curvature. The endpoint of a branch of the \mathcal{SS} .

An $A_1 A_2$ point: the midpoint of a circle tangent at two distinct points of the shape but located at the evolute. A turning point on the \mathcal{SS} .

An A_1^3 point: the midpoint of one circle tangent at three distinct points of the shape. An intersection of three branches of the \mathcal{SS} .

An A_1^2 / A_1^2 point: the midpoints of two circles with different radii coincide and two branches of the \mathcal{SS} intersect.

These points can be seen in Figure 1.2a,b.

1.2.2 Transitions

In the following we briefly state the possible transitions of the \mathcal{SS} . For more details and figures the reader is referred to [3, 15].

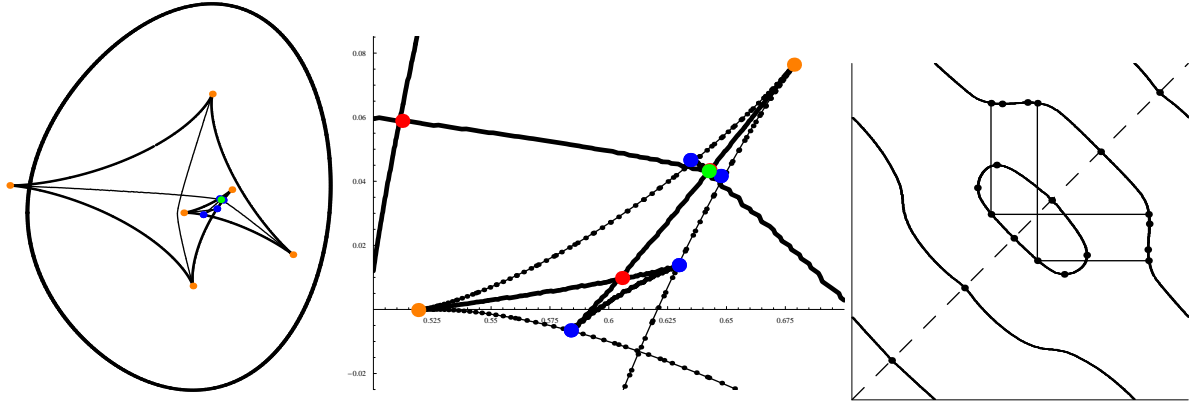


Figure 1.2: a) A shape (thickest), its evolute (thick) and the \mathcal{SS} with special points b) Close up. c) Pre- \mathcal{SS} .

At an A_1^4 transition a collision of A_1^3 points appears. Before and after the transition four A_1^3 points occur and the \mathcal{SS} doesn't change. The result on the \mathcal{MA} , however, is a reordering of the connections of two connected Y-parts of the skeleton.

At an A_1A_3 transition, a cusp of the evolute (and thus an end part of a \mathcal{SS} branch including an A_3 point) intersects a branch of the \mathcal{SS} and an A_1^3 point as well as two A_1A_2 points are created or annihilated. The A_1^3 point lies on the A_3 containing branch, while the other branch contains a "triangle" with the A_1^3 and the A_1A_2 's as corner points.

The A_4 transition corresponds to creation or annihilation of a swallowtail structure of the evolute and the creation or annihilation of the enclosed \mathcal{SS} branch with two A_3 and two A_1A_2 points.

At an $A_1^2A_2$ transition two non-intersecting A_1A_2 -containing branches meet a third \mathcal{SS} branch at the evolute, creating or annihilating two situations where three different branches intersect at two A_1^3 points.

The A_2^2 moth transition describes the creation or annihilation of a \mathcal{SS} branch containing only four A_1A_2 and no A_3 points. These points lie pair wise on two opposite parts of the evolute. Each point is connected via the \mathcal{SS} to the two points on the opposite part of the evolute.

When going through an A_2^2 nib transition, two branches of the \mathcal{SS} , each containing an A_1A_2 point, meet and exchange a sub-branch.

1.3 Pre-Symmetry Set

The pre- \mathcal{SS} is obtained by visualizing the Symmetry Set in parameter space, so essentially it is visualizing the zero crossings of $(p_i - p_j) \cdot (\mathcal{N}_i \pm \mathcal{N}_j)$. This is done in Figure 1.2b. On the axis one finds the parameters p_i and p_j . The black curved lines represent the zero crossings.

Firstly, it needs to be remarked that the diagram repeats across its borders: the parameter moves along a closed curve. So the diagram represents a torus. Furthermore, the axis are to be identified, since they both relate to the same parameter along the shape. So the image is symmetric in the diagonal and the plot represents in fact a Möbius strip, with the diagonal as its boundary. In Figure 1.2c, one can see two curves ranging over the entire domain and one closed loop.

1.3.1 Points on the Pre-Symmetry Set

Since curves in the pre- \mathcal{SS} generically don't intersect, one easily obtains separate branches. On these branches the points are classified as follows:

At A_3 points, one has $p_i = p_j$. They are located at the diagonal since they don't concern two different points on the shape.

At A_1A_2 points the \mathcal{SS} hits the evolute and is reflected. This implies that one of the two involved points is also reflected. The pre- \mathcal{SS} therefore has a horizontal or vertical tangent (identical due to symmetry in the

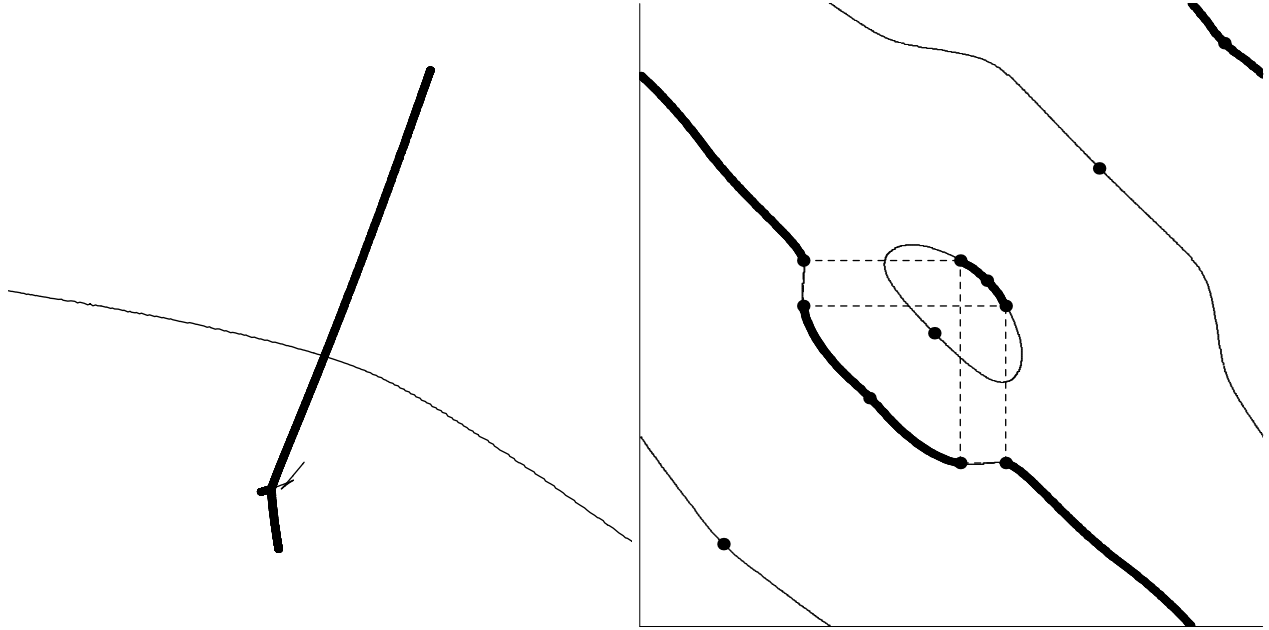


Figure 1.3: MA in the (Pre-) Symmetry Set.

diagonal).

At an A_1^3 point three parts of the SS intersect. In the pre- SS these points are detectable as the occurrence of the triple point sets (p_1, p_2) , (p_1, p_3) , and (p_2, p_3) (and, of course, the diagonal symmetric counterpart). This is visualized by the box-set in Figure 1.2b and c.

All other points are A_1^2 points.

The \mathcal{MA} also lives in the pre- SS space, see Figure 1.3. It starts at a diagonal point, moves along a curve until an A_1^3 point is encountered (a Y-junction of the skeleton). There it jumps to the branch to which the box is connected. There it continues until another A_1^3 point is encountered. This may be the same as before, but in mirrored sense. Hence the \mathcal{MA} -walk went to an endpoint of the skeleton and returned. Finally, the tour ends in the starting diagonal point and the \mathcal{MA} has been traversed twice, starting and ending in an endpoint.

1.4 Transitions of the pre-symmetry set

The list of transitions valid for the SS , also apply to the pre- SS . In the following we state the consequences of these events for the pre- SS . Firstly, branches can be created or annihilated in the pre- SS . They can be qualified on- and of-diagonal. Secondly, curves in the pre- SS can be smoothed (or pronounced). This relates to the annihilation or creation of pairs of local extrema on them. Thirdly, curves can meet and exchange branches. Finally, two types of special constellations of A_1^3 -points can occur, one being related to the creation or annihilation of two A_1^3 -points.

1.4.1 Curves on the diagonal: A_4

The A_4 transition (Figure 1.4) corresponds to creation or annihilation of a closed loop on the diagonal, thus containing two A_3 points on the diagonal and two A_1A_2 points as the horizontal and vertical tangents (note that the diagonal is a axis of symmetry).

1.4.2 Curves of the diagonal: A_2^2 moth

When going through an A_2^2 nib transition (Figure 1.5), a closed of-diagonal loop is created or annihilated. It cannot intersect the diagonal. Note that in the visualization two loops occur due to diagonal symmetry.

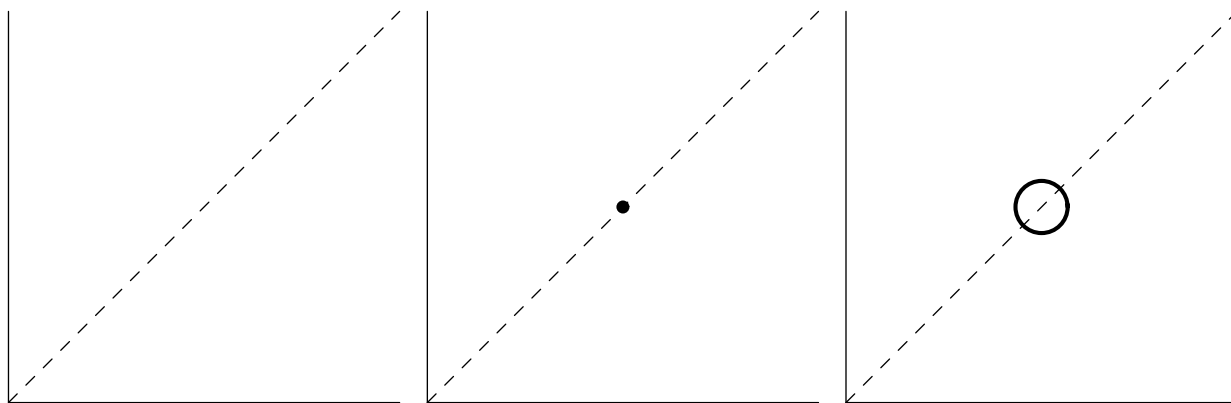


Figure 1.4: A_4 transition in the Pre-Symmetry Set.

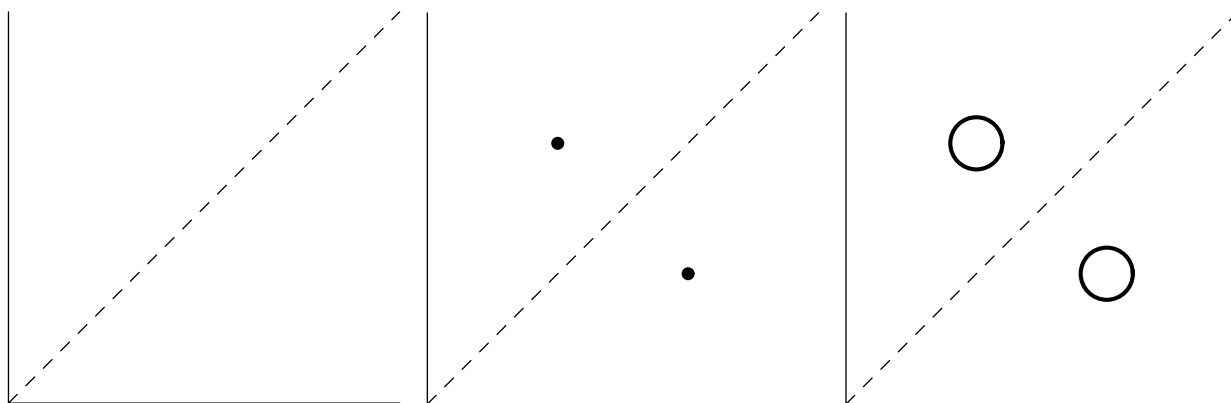


Figure 1.5: A_2^2 -moth transition in the Pre-Symmetry Set.

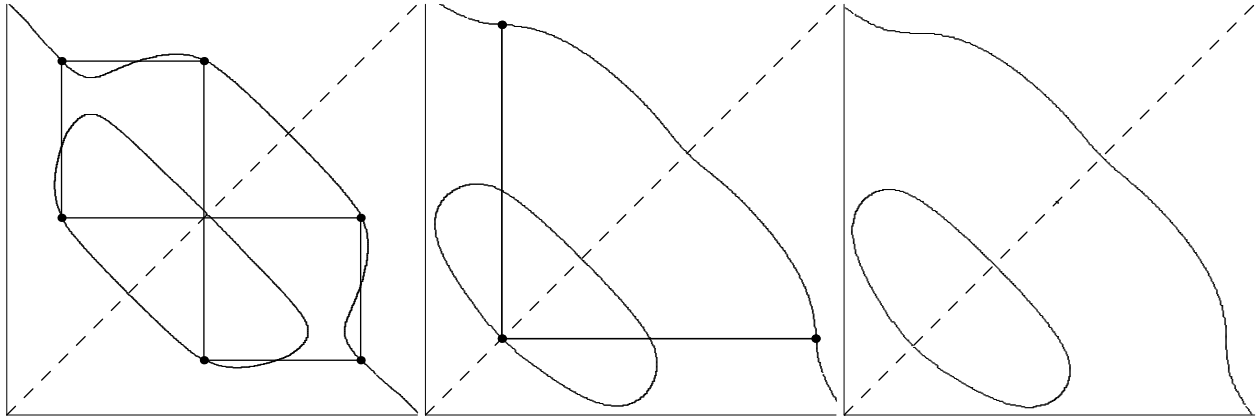


Figure 1.6: A_1A_3 transition in the Pre-Symmetry Set.

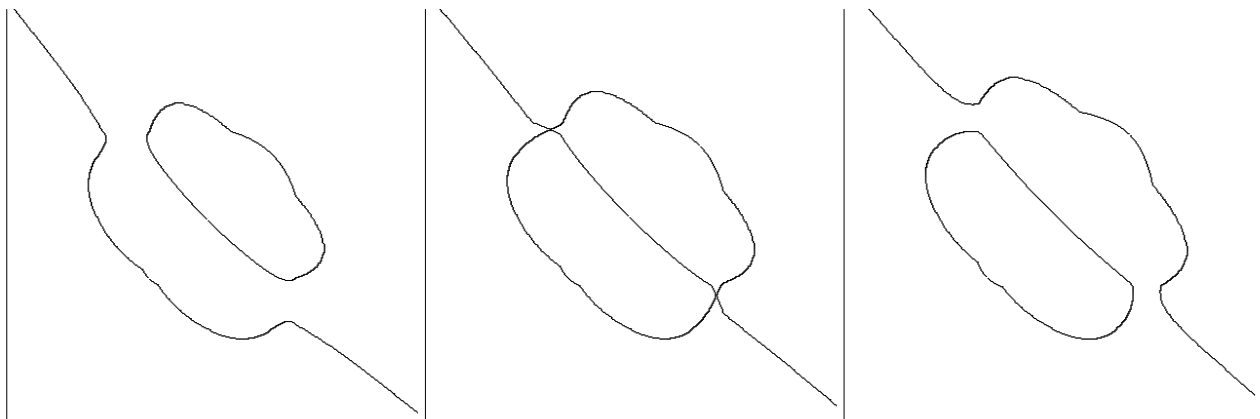


Figure 1.7: A_2^2 -nib transition in the Pre-Symmetry Set.

1.4.3 Smoothing curves: A_1A_3

At an A_1A_3 transition (Figure 1.6), one curve goes through an inflection point and changes from zero to two local extrema (horizontal or vertical tangents) - which are A_1A_2 points. Outside the two extrema two positions of the A_3 are located, the third one is located on the curve that represents the other SS -branch involved in the interaction.

1.4.4 Swapping of branches: A_2^2 nib

When going through an A_2^2 nib transition (Figure 1.7), two branches approach with their local A_1A_2 points with the same kind of tangent. They meet, forming an intersection, exchanging connection and afterwards they move away with again the same kind of tangent, but opposite to the one before (horizontal vs. vertical, or vice versa).

1.4.5 Collision of four A_1^3 - points: A_1^4

At an A_1^4 transition (Figure 1.8) a collision of four A_1^3 points appears. This implies that in the pre-ss four box-sets, each combining the three positions out of (p_1, p_2, p_3, p_4) and six pairs (p_i, p_j) , coincide. Before and after the transition there are four boxes / twelve pairs of points on six curve parts, on each of them two A_1^3 . The only thing that changes is the position of the A_1^3 points on each curve.

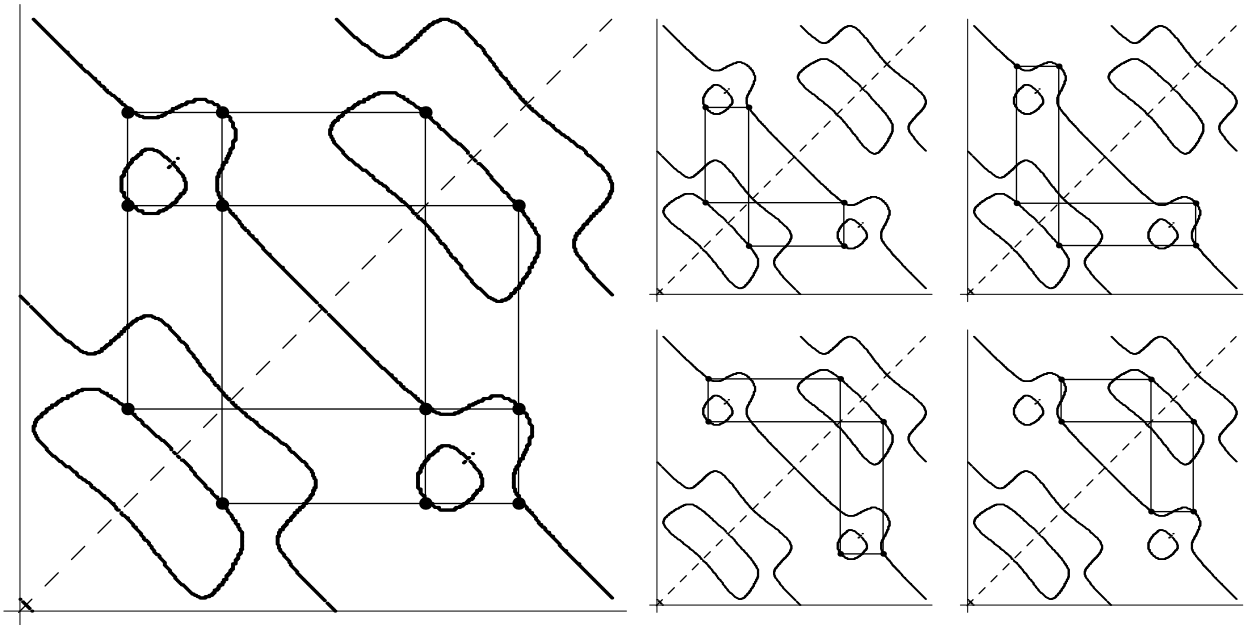


Figure 1.8: A_1^4 transition in the Pre-Symmetry Set.

1.4.6 (Dis)appearance of two A_1^3 -points: $A_1^2 A_2$

At $A_1^2 A_2$ transition (Figure 1.9) two A_1^3 -points are created or annihilated at two $A_1 A_2$ points. So two box-sets meet or emerge at the two $A_1 A_2$ points at (p_1, p_2) and (p_1, p_3) , and at (p_2, p_3) on a third branch. So necessarily each $A_1 A_2$ point needs to be surrounded by the two A_1^3 points.

1.5 Summary and Conclusions

In this paper we presented a new way and powerful tool to visualize changes of the Symmetry Set. The method depends on the pre- \mathcal{SS} , which is the \mathcal{SS} in the parameter space. We listed the possible changes of the pre- \mathcal{SS} , derived from those for the \mathcal{SS} and gave examples how they look like. They relate to annihilation or creation of curves in the pre- \mathcal{SS} , smoothing of them, exchanging sub-branches, and interactions of A_1^3 -points.

Besides these transitions we gave an example of the presence of the Medial Axis in both the \mathcal{SS} and the

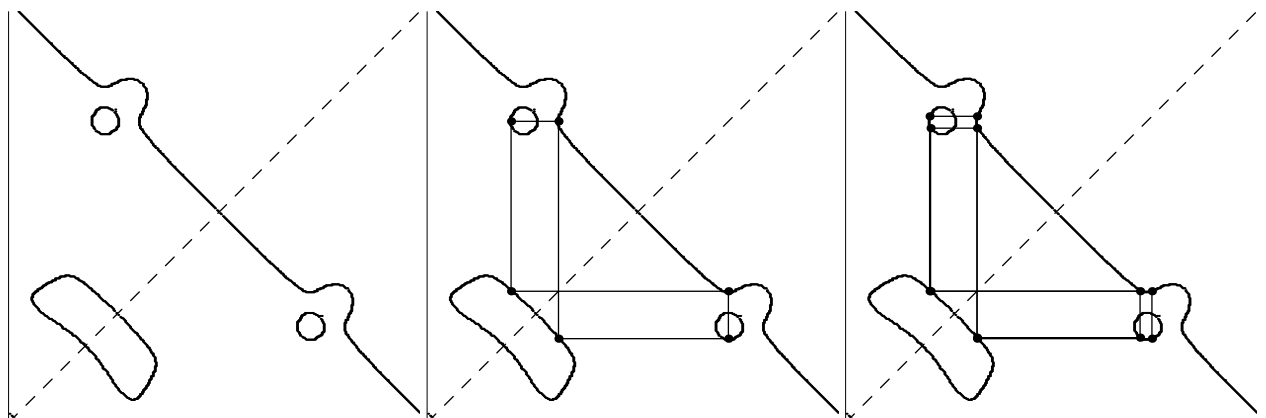


Figure 1.9: $A_1^2 A_2$ transition in the Pre-Symmetry Set.

pre- \mathcal{SS} . Although the structure of the pre- \mathcal{SS} is hardly affected by the transitions involving A_1^3 -points, the \mathcal{MA} is.

The knowledge of these changes can be used to change the pre- \mathcal{SS} accordingly and so smoothing and/or simplifying the pre- \mathcal{SS} and thus the \mathcal{SS} and its data structure [28]. This includes in the pre- \mathcal{SS} removal of fine and complicated details, as well as editing of global structures. For the \mathcal{SS} this yields removal of points and structures 'far away' from the shape, as well as simplification of the \mathcal{SS} branches and its data structure [28]. By selecting branches in the pre- \mathcal{SS} one can select branches of the \mathcal{SS} .

Acknowledgements

The authors thank Prof. Giblin from Liverpool University for fruitful discussions.

Chapter 2

Amending the pre-Symmetry Set

Abstract

The Symmetry Set (SS) and its representation in parameter space, the pre-Symmetry Set, can be used to describe a shape with a data structure that is related to the so-called arc-annotated sequence. Operations on it have a complexity less than that on graph-structures, obtained by the Medial Axis (a subset of the SS). Changes in the data structure and the Pre-SS are directly related to so-called transitions (topological changes) of the SS. In this paper we discuss the abilities of the pre-SS and parts of it, in describing the shape. By editing the pre-SS, the SS and the data structure can be simplified, for example for smoothing or simplifying purposes.

2.1 Introduction

In shape analysis, much effort has been put into the research on the skeleton, or Medial Axis [2], as a way to represent the shape in a more simplified way. As it was soon realized, the Medial Axis itself didn't carry enough information [14] and sophisticated extensions were built, like the Shock Graph method [41]. Basically, each point on the Medial Axis is endowed with some augments related to the distance to the shape itself or related to its neighbours. Next, the potential changes of the Medial Axis were investigated, yielding a set of possible transition [15]. In that way different shapes can be related to each other for shape indexing and retrieval [35, 39].

The results on transitions boiled down from the results on the possible transitions of the Symmetry Set. This set, containing the Medial Axis as subset, has been thoroughly studied in [4]. Its transitions are described in [3]. The Symmetry Set has its advantage in being easily described in mathematical sense, but its visualization is less pleasant for the eye. So most of the research has been focused on the (augmented) Medial Axis.

Recently, however, a data structure was presented for the Symmetry Set [], that can be visualized by a sequence of nodes, that are pair wise joined. This structure is related to the arc-annotated sequence [1] used in RNA research. Its main advantage over the graph structure used for the Medial Axis is that it allows operations on it with a lower complexity.

In this paper we present a way to visualize the Symmetry Set in a more pleasing manner, by using the pre-Symmetry Set. Here we use pairs of points on the shape that give rise to a Symmetry Set point. So this avoids precise calculation of the Symmetry Set points in the plane. Secondly, it has the nice property that parts with small support remain small in the visualization. So a small perturbation of the shape gives a small perturbation in the set.

We also present the possible transitions of the pre-Symmetry Set and discuss how this can be used to amend the (pre-) Symmetry Set. In this way the original shape can be locally smoothed.

2.2 Symmetry Set

The Symmetry Set is defined as the closure of the loci of the circles tangent to a shape. See Figure 2.1. The

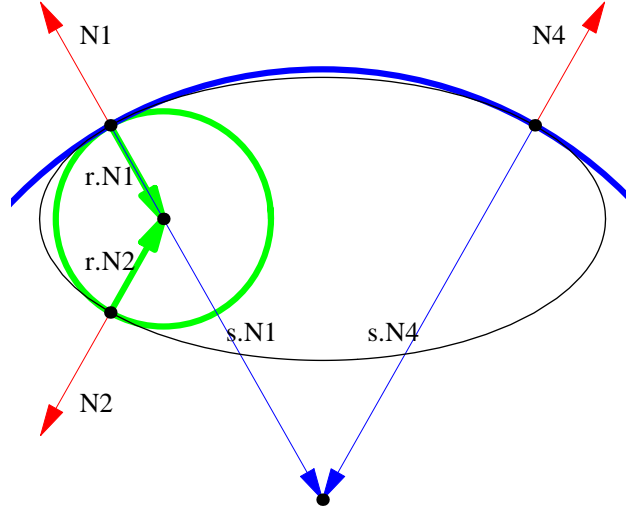


Figure 2.1: Definition of the Symmetry Set. See text for details.

shape is given by the oval. Inside a circle is tangent to it at two locations, so the *unit* normals \mathcal{N}_1 and \mathcal{N}_2 are equal for the shape and the circle. The centre of the circle is found by multiplying minus the radius r with the normals. Note that this is also a Medial Axis point. Next, also outside a circle is tangent to the shape at two locations, where the unit normals \mathcal{N}_3 and \mathcal{N}_4 are equal for the shape and the circle.

From this image it follows immediately that a point on the shape relates to at least two points on the Symmetry Set, in contrast with the Medial Axis. A recipe for finding the Symmetry Set is the given by the following observations.

Let a circle be tangent to the shape as in Figure 2.2a. Then call the points at which it is tangent p_1 and p_2 (Figure 2.2b). Then the vector $p_1 - p_2$ is perpendicular to the vector $\mathcal{N}_1 + \mathcal{N}_2$ when the circle is tangent twice from the same side as shown in these images, or to the vector $\mathcal{N}_1 - \mathcal{N}_2$, when tangent from two different sides (see [15]). So to find these locations it suffices to have a point p_i fixed and try all other points p_j along the shape and find zerocrossings of

$$(p_i - p_j) \cdot (\mathcal{N}_i \pm \mathcal{N}_j) \quad (2.1)$$

Next, the centre of the circle - the location of the Symmetry Set point - is given by

$$p_i - r\mathcal{N}_i = p_j \pm r\mathcal{N}_j \quad (2.2)$$

Another tool that is used in the analysis of the Symmetry Set is the evolute. Let κ be the curvature of the shape \mathcal{S} , in parametrised form $\kappa(t) = (x_t y_{tt} - y_t x_{tt}) / (x_t^2 + y_t^2)^{-3/2}$, or $\kappa(x, y) = -(L_x^2 L_{yy} - 2L_x L_y L_{xy} + L_y^2 L_{xx}) / (L_x^2 + L_y^2)^{-3/2}$ in spatial coordinates, the the evolute is given by $\mathcal{S} + \mathcal{N} / \kappa$. In Figure 2.2c the ellipse, its evolute and its Medial Axis (horizontal line) and Symmetry Set (both lines) are shown.

2.2.1 Points on the Symmetry Set

Due to the geometry of the shape and the order of tangency, five distinct types of points generically occur on the Symmetry Set [4]. They are:

- An A_1^2 point: the "common" midpoint of a circle tangent at two distinct points of the shape.
- An A_3 point: the midpoint of a circle located at the evolute and tangent at the point of the shape with the local extremal curvature. The endpoint of a branch of the \mathcal{SS} .

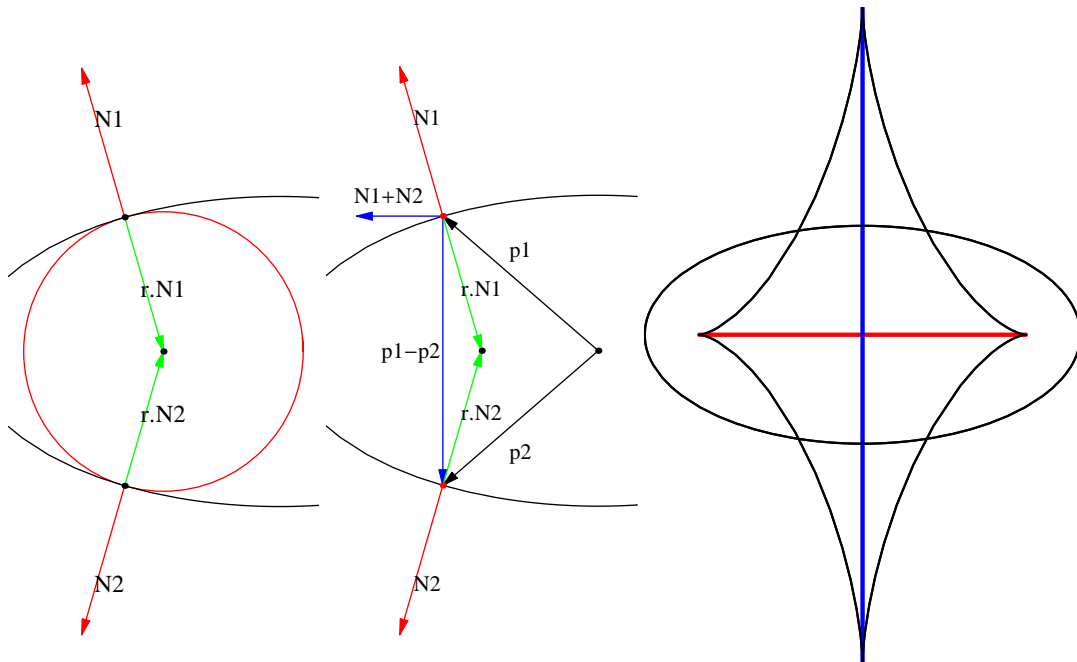


Figure 2.2: Deriving the Symmetry Set. See text for details.

- An A_1A_2 point: the midpoint of a circle tangent at two distinct points of the shape but located at the evolute. A turning point on the SS .
- An A_1^3 point: the midpoint of one circle tangent at three distinct points of the shape. An intersection of three branches of the SS .
- An $A_1^2A_1^2$ point: the midpoint of two circles tangent at two pairs of distinct points of the shape with different radii. Since this produces only an intersection due to projection on the plane, it is omitted in the forth going.

They are important, since transitions occur in special arrangements of points.

2.2.2 Transitions

In the following we briefly state the possible transitions of the SS . For more details the reader is referred to [3].

A_1^4

At an A_1^4 transition a collision of A_1^3 points appears. Before and after the transition six lines, four A_1^3 points occur. The result on the \mathcal{MA} is a reordering of the connections of two connected Y-parts of the skeleton. For the SS , however, the Y-parts are the visible parts of SS branches going through A_1^3 points. So for the SS representation nothing changes.

A_1A_3

At an A_1A_3 transition, a cusp of the evolute (and thus an endpoint of a SS branch including a A_3 point) intersects a branch of the SS and an A_1^3 point as well as two A_1A_2 points are created or annihilated. The A_1^3 point lies on the A_3 containing branch, while the other branch contains a "triangle" with the A_1^3 and the A_1A_2 's as corner points.

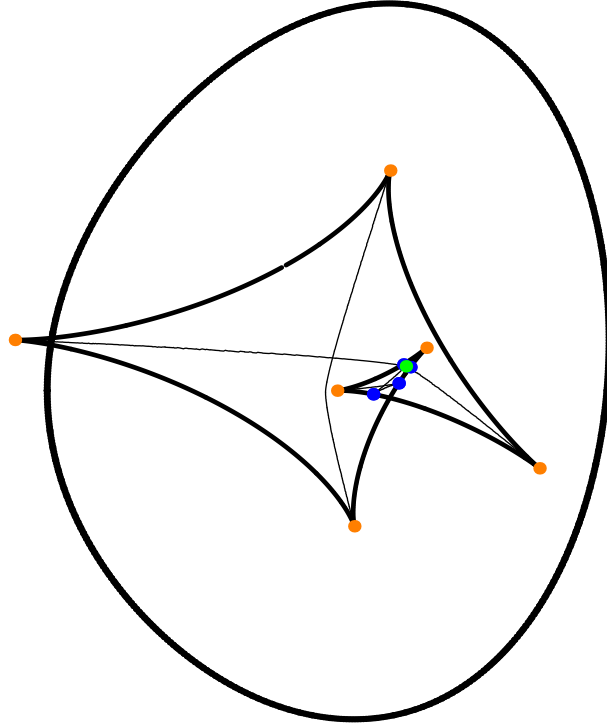


Figure 2.3: Shape and the Symmetry Set with special points

A_4

The A_4 transition corresponds to creation or annihilation of a swallowtail structure of the evolute and the creation or annihilation of the enclosed SS branch with two A_3 and two A_1A_2 points.

$A_1^2A_2$

At an $A_1^2A_2$ transition two non-intersecting A_1A_2 -containing branches meet a third SS branch at the evolute, creating two times three different branches intersecting at two A_1^3 points. Or the inverse transition occurs.

A_2^2 moth

The A_2^2 moth transition describes the creation or annihilation of a SS branch containing only four A_1A_2 and no A_3 points. These points lie pairwise on two opposite parts of the evolute. Each point is connected via the SS to the two points on the opposite part of the evolute.

A_2^2 nib

When going through an A_2^2 nib transition, two branches of the SS , each containing an A_1A_2 point, meet and exchange a subbranch.

2.3 Pre-Symmetry Set

The pre- SS is obtained by visualizing the Symmetry Set in parameter space, so essentially it is visualizing the zerocrossings of Eq. 2.1. This is done in Figure 2.4.

On the axis one finds the parameters p_i and p_j . The black curved lines represent the zerocrossings.

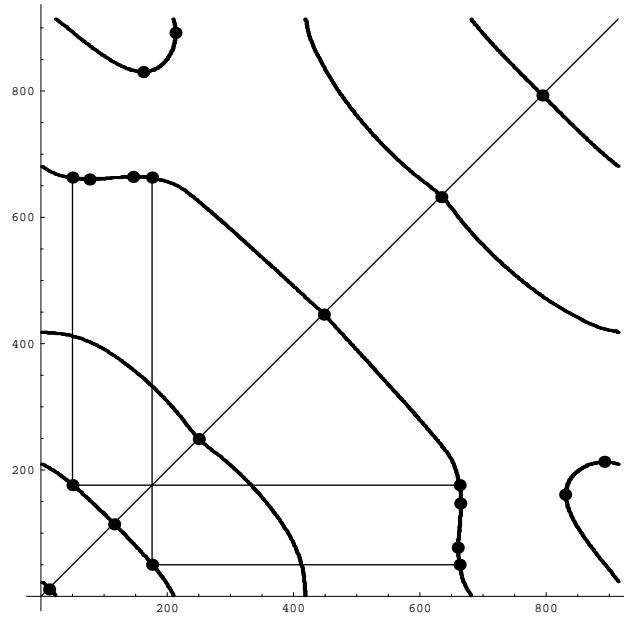


Figure 2.4: Visualizing the Pre-Symmetry Set. See text for details.

Firstly, it needs to be remarked that the diagram repeats across its borders: the parameter moves along a closed curve. So the diagram represents a torus. Furthermore, the axis are to be identified, since they both relate to the same parameter along the shape. So the image is symmetric in the diagonal and the plot represents in fact a Moebius strip, with the diagonal as its boundary.

In this Figure, one can see two curves ranging over the entire domain and one closed loop (bottom left with parts bottom right and (the symmetric counterpart) top left).

2.3.1 Points on the Pre-Symmetry Set

Since curves in the pre- SS don't intersect, one easily obtains separate branches. On these branches the points are classified as follows:

- A_3 : At A_3 points, one has $p_i = p_j$, since they are located at the diagonal and don't concern two different points on the shape.
- A_1A_2 : At A_1A_2 points the SS hits the evolute and is reflected. This implies that one of the two involved points, say p_i , is also reflected. The pre- SS therefore has a horizontal or vertical tangent.
- A_1^3 : At an A_1^3 point three parts of the SS intersect. In the pre- SS these points are detectable as the occurrence of the triple pointsets (p_1, p_2) , (p_1, p_3) , and (p_2, p_3) (and, of course, its diagonal symmetric counterpart). This is visualized by the box-set in Figure 2.4.
- A_1^2 : All other points are A_1^2 points.

2.3.2 Transitions

The list of transitions valid for the SS , also apply to the pre- SS . In the following we state the consequences of these events for the pre- SS .

A_1^4

At an A_1^4 transition a collision of A_1^3 points appears. This implies that in the pre-ss four box-sets, each combining the three positions, coincide. Before and after the transition there are six curves with, each of them two A_1^3 . The only thing that changes is the ordering of each pair of A_1^3 points on each curve. This boils down to inverting the order of the four box-sets.

A_1A_3

At an A_1A_3 transition, one curve goes through an inflection point and changes from zero to two local extrema (horizontal or vertical tangents) - which are A_1A_2 points. Outside the two extrema two positions of the A_3 are located, the third is located on the curve that represents the other SS -branch involved in the interaction.

A_4

The A_4 transition corresponds to creation or annihilation of a closed loop on the diagonal in the pre- SS , thus containing two A_3 points on the diagonal and two A_1A_2 points as the horizontal and vertical tangents (note that the diagonal is a axis of symmetry).

$A_1^2A_2$

At an $A_1^2A_2$ transition two branches with each an A_1A_2 point surrounded by two A_1^3 points meet and leave without the A_1^3 points. The A_1A_2 points have the same tangent. On a third branch two A_1^3 points meet and vanish. Or, of course, the opposite (creation) event occurs.

A_2^2 moth

When going through an A_2^2 nib transition, a closed of-diagonal loop is created or annihilated in the Pre- SS . It cannot intersect the diagonal. Note that in the visualization also a loop occurs due to mirroring in the diagonal.

A_2^2 nib

When going through an A_2^2 nib transition, two branches approach with their local A_1A_2 points with the same kind of tangent. They meet, forming an intersection, exchanging connection and afterwards they move away with again the same kind of tangent, but opposite to the one before (horizontal vs. vertical, or vice versa).

2.4 Amending the pre-ss

Since the distinct curves of the pre- SS resemble distinct branches of the SS , editing the pre- SS directly implies editing the SS . In order to avoid arbitrary changes, one should amend according to the transitions as given above. Furthermore, creating new structures is mostly not wanted since it complicates the SS . And finally, when amending, one usually wants to smooth local structures. So when removing structures, they should not be too large.

2.4.1 Smoothing the pre-ss branches

To simplify the SS in a predefined manner, one can apply the A_2^2 moth to remove of-diagonal loops and the A_4 to remove on-diagonal loops. This resembles removal of a branch of the SS . Applying the A_1A_3 yields removal of local humps, that is: a pair of A_1A_2 points, together with an A_1^3 point. An example of the latter is given in Figure 2.5.

On the left, a part of Figure 2.4 is taken with 2 A_1A_2 points. Smoothing this part yields removal of the A_1A_2 parts. In the SS this relates removing a swallowtail part.

Applying the A_1A_3 and the A_4 , the SS and pre- SS change as shown in Figure 2.6.

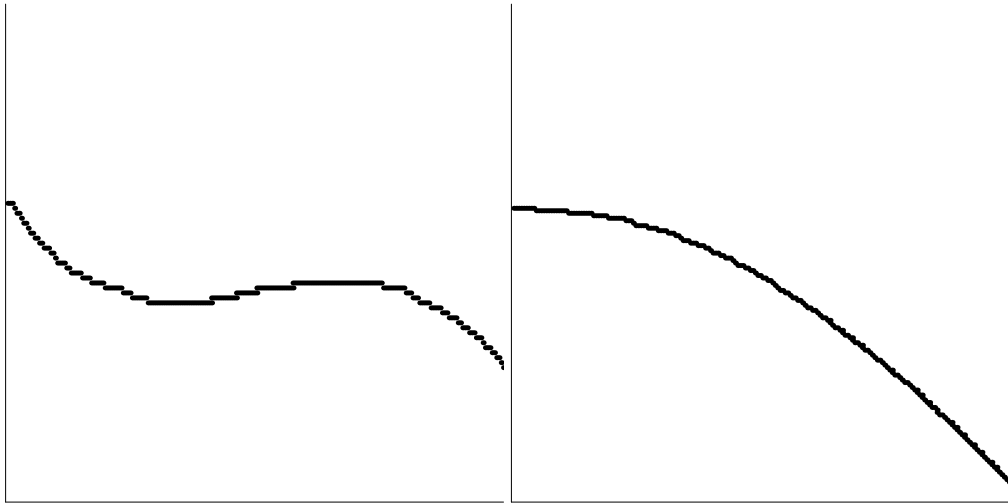


Figure 2.5: Amending the Pre-Symmetry Set

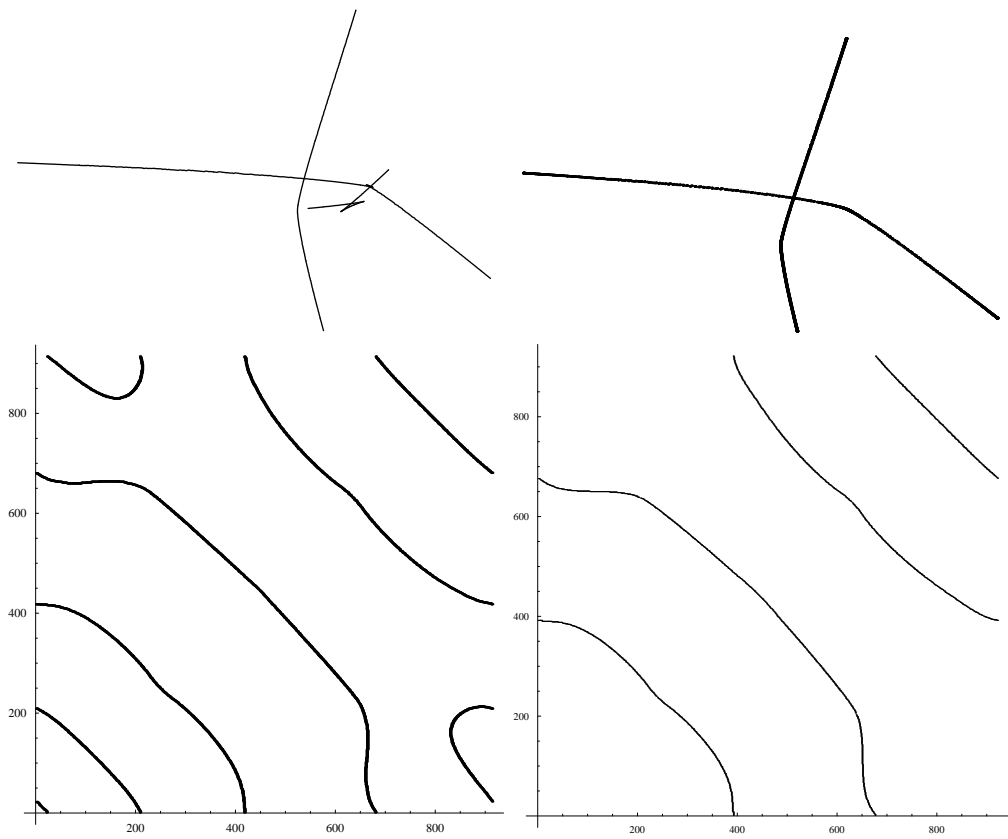


Figure 2.6: Amending the Pre-Symmetry Set: Results on the SS (top) and the $Pre-SS$ (bottom).

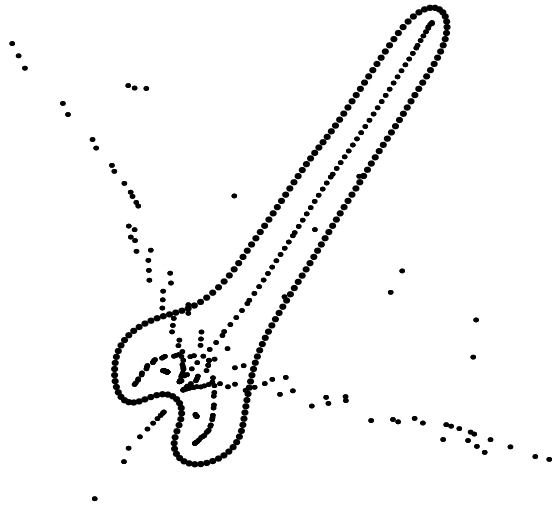


Figure 2.7: Tool-shape and its \mathcal{SS} .

2.4.2 Selecting pre-ss branches

As a more real example, see the shape of a tool in Figure 2.7. The points of the shape are the thick dots. The thin dots are the points of the Symmetry Set. Due to concavities, points can lie at infinity (i.e. where the curvature is zero). The Symmetry Set thus consists of lines through infinity. Therefore, the Symmetry Set itself is not really pleasant for the eye.

Considering the pre- \mathcal{SS} , Figure 2.8, these infinity problems are avoided. In fact, of the twelve curves present in the pre-ss, nine only relate to points 'far away'.

When the pre- \mathcal{SS} branches are sorted on their length - i.e. largest support -, the three not-only-far-away branches relate to the first three pre- \mathcal{SS} branches. The are, together with their \mathcal{SS} counterparts, depicted in Figure 2.9.

One can observe that the first branch relates to the 'symmetry line' in the shape from top-left to bottom right. Considering the second and third branch, one obtains Figure 2.10. Here we see a Simplified Symmetry Set that is in between the Symmetry Set and the Medial Axis.

Similarly, when considering the fish of Figure 2.11, with its \mathcal{SS} and pre- \mathcal{SS} , one can select proper pre- \mathcal{SS} branches, in this case 1 and 5 of the 34 present, see Figure 2.12, to visualize a simplified \mathcal{SS} as shown in Figure 2.13.

One can see that branch 1 represents the main axis of the fish. In the middle, a lot of extra structure is present due to the fins. This extra structure is clearly visible in the pre- \mathcal{SS} . It can be removed by further amending the pre- \mathcal{SS} .

2.5 Summary and Conclusions

In this paper we presented a new way and powerful tool to visualize and edit the Symmetry Set. The method depends on the pre- \mathcal{SS} , which is the \mathcal{SS} in the parameter space. This avoids the problem that branches of the \mathcal{SS} go to infinity if the curvature on the shape is zero. By selecting branches in the pre- \mathcal{SS} one can select branches of the \mathcal{SS} . By the presented transitions for the pre- \mathcal{SS} , derived from those for the \mathcal{SS} , one can amend the pre- \mathcal{SS} and thus the \mathcal{SS} . This includes in the pre- \mathcal{SS} removal of fine and complicated details, as well as editing of global structures. For the \mathcal{SS} this yields removal of points and structures 'far away' from the shape, as well as simplification of the \mathcal{SS} branches.

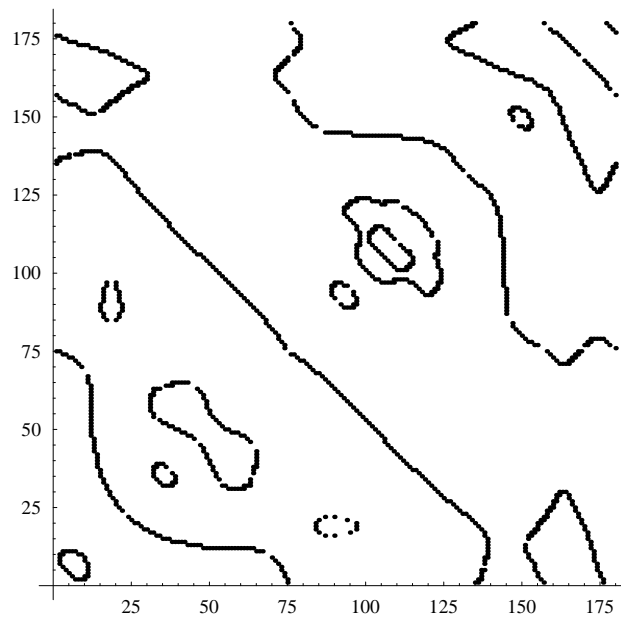


Figure 2.8: Pre-SS of the tool.

As a result, one ends up with a structure that can be considered as a Simplified Symmetry Set, being in between the Medial Axis and the Symmetry Set. Secondly, it relates directly to simplifying the arc-annotated sequence-like data structure as proposed in [], allowing simpler data structures.

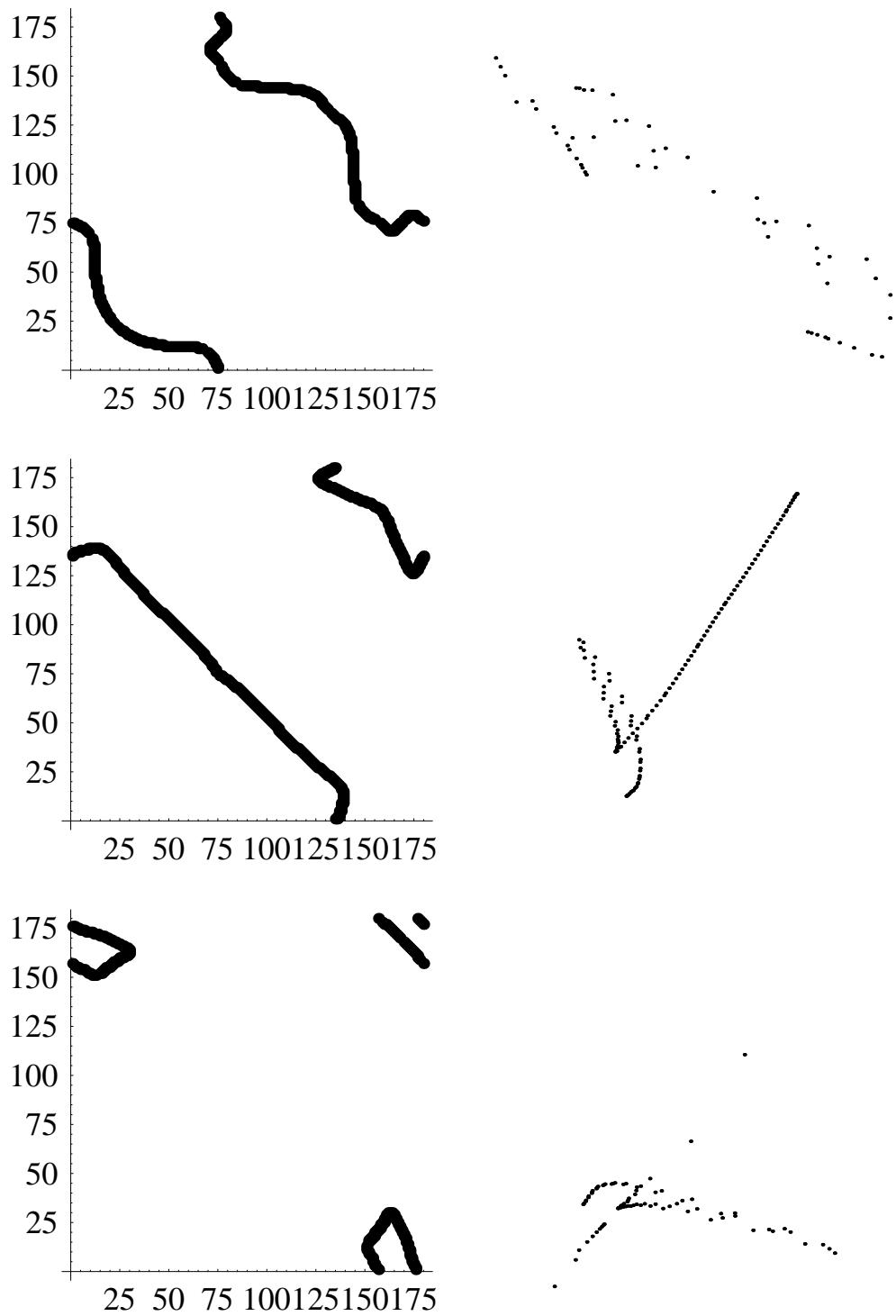


Figure 2.9: First three branches of the Pre-Symmetry Set (left) and SS (right).

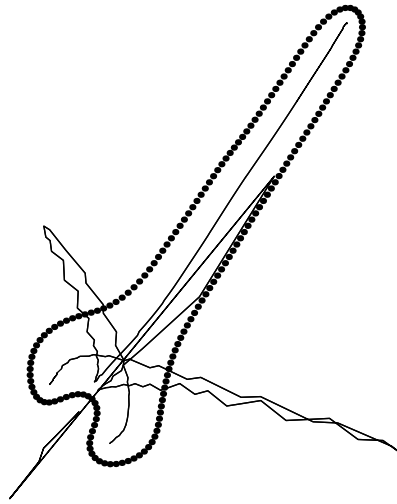


Figure 2.10: Simplified SS of the tool.

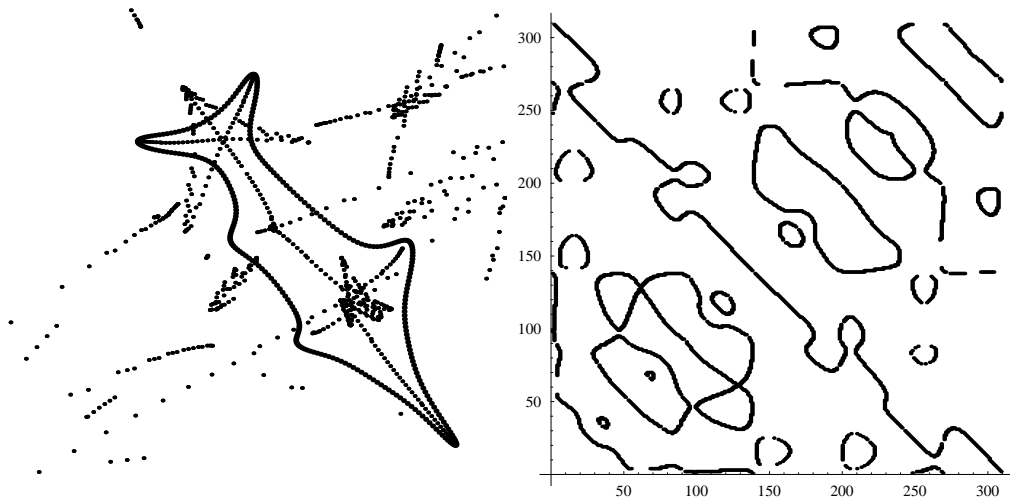


Figure 2.11: Left: Fish, with its SS . Right: $Pre-SS$ of the fish.

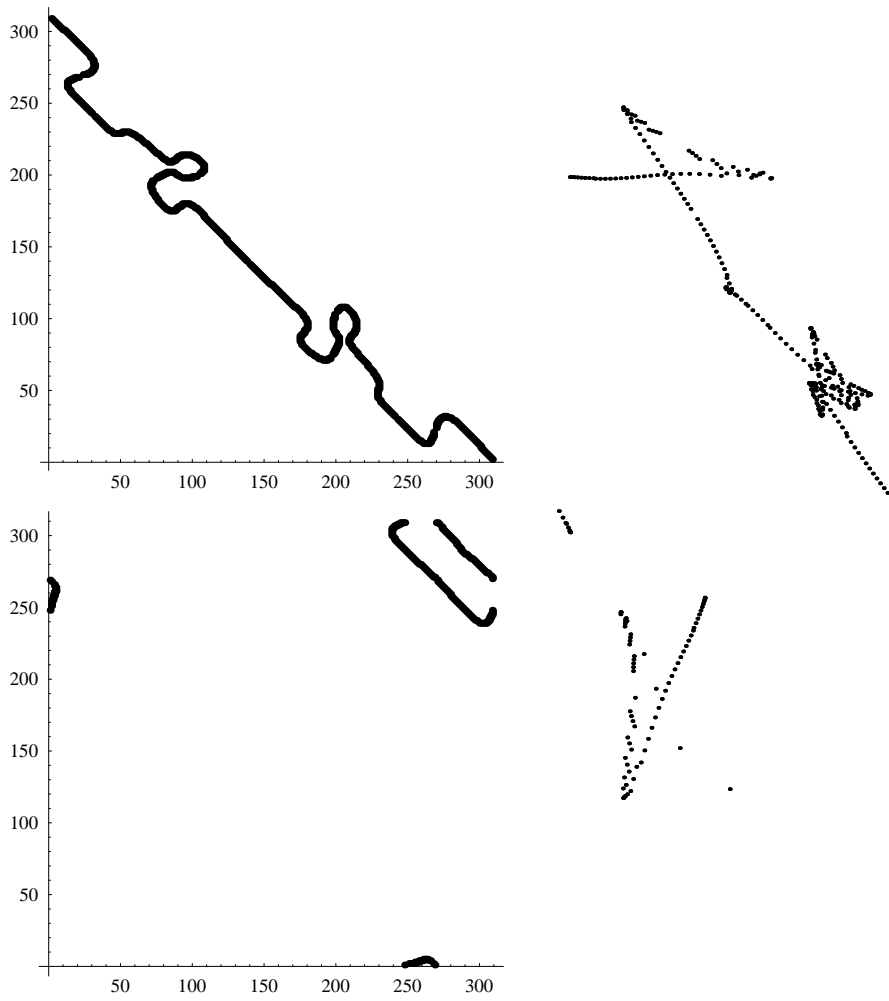


Figure 2.12: Selecting Pre-Symmetry Set branches and their related SS branches: branch 1 (top) and branch 5 (bottom) of the fish.

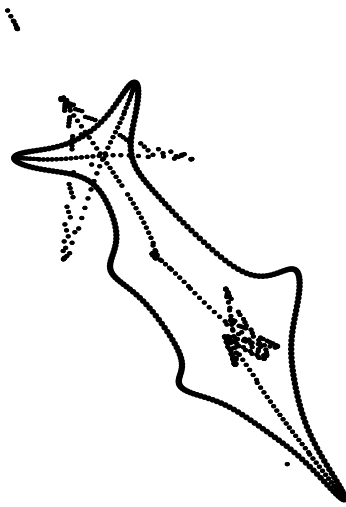


Figure 2.13: Simplified SS of the fish using only the branches 1 and 5.

Chapter 3

Geometric Skeletonization

Abstract

In this paper we present a method to derive the skeleton of a shape by means of its Symmetry Set. We use the property that the Medial Axis is a subset of the Symmetry Set, the latter being the midpoints of circles tangent to a shape at at least two points, the former those circles that do not contain other circles, the so-called maximal circles. The Symmetry Set points are derived by means of zero crossings of two equations, based on geometric arguments.

3.1 Introduction

The skeleton of a shape is defined by the set of points that have at least two different points on the shape as closest points. It is a well-known aspect of a shape that carries information in an easier way [2]. In order to derive the skeleton several different approaches are proposed. The first methods detects ridges, or singularities of the distance map of points on the shape. [7, 40, 43] Secondly, Voronoi diagram can be used [20, 34, 44]. Thirdly, by simulating a grass-fire flow [30, 42], thinning [6] of the object bounded by the shape, is preformed. Although all methods perform theoretically similar, on real discrete shapes the outcome may be different.

In this paper we propose a method based on the geometry that is embedded in the definition of the skeleton. If two points are the closest points, they actually lie on a circle tangent to the shape at these points, while its midpoint is the skeleton point.

A little geometry based on this tangency aspect, together with the locations of the points give a methodology to find the skeleton point, as described in section 3.2. It actually gives more than the skeleton, viz. the Symmetry Set, but a more careful inspection of the collection of points reveals a simple method to extract the skeleton points.

3.2 Background

In this section we describe the geometric tools Symmetry Set, Medial Axis and the pre-Symmetry Set.

3.2.1 Medial Axis and Symmetry Set

The Symmetry Set is defined as the closure of the loci of the circles tangent to a shape [4, 15]. The Medial Axis is the subset containing maximal circles (i.e. those circles that contain no other circles).

Let a circle be tangent to the shape as in Figure 3.1b. Then call the points at which it is tangent p_1 and p_2 . Then the vector $p_1 - p_2$ is perpendicular to the vector $\mathcal{N}_1 + \mathcal{N}_2$ when the circle is tangent twice from the same side as shown in these images, or to the vector $\mathcal{N}_1 - \mathcal{N}_2$, when tangent from two different sides (see [15]). So to find these locations it suffices to have a point p_i fixed and try all other points p_j along the shape and find zero crossings of

$$(p_i - p_j) \cdot (\mathcal{N}_i \pm \mathcal{N}_j) \tag{3.1}$$

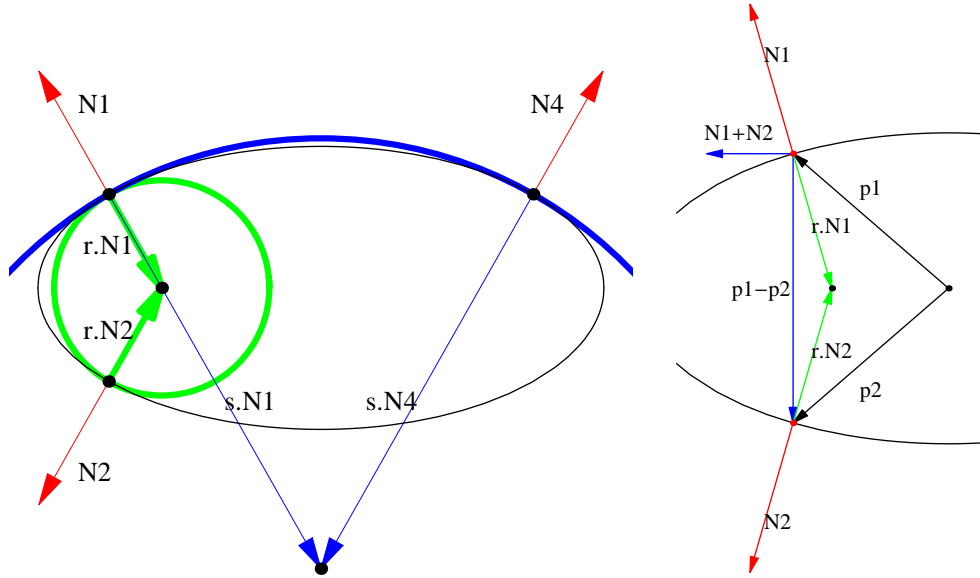


Figure 3.1: a) Circles tangent to a shape b) Computing the Symmetry Set (see text).

Next, the centre of the circle - the location of the SS point - is given by

$$p_i - r\mathcal{N}_i = p_j \pm r\mathcal{N}_j \quad (3.2)$$

If the normal vectors are parallel for a pair of shape points, the set of points obtained as the midpoints of these two points on the shape is called Anti-Symmetry Set. Another tool that is used in the analysis of the SS is the evolute. Let κ be the curvature of the shape \mathcal{S} , then the evolute is given by $\mathcal{S} + \mathcal{N}/\kappa$. In Figure 3.2a a shape, its evolute (thick line connecting endpoints in cusps) and the SS (both lines) are shown. Its \mathcal{MA} is the vertical curve.

3.2.2 Points on the Symmetry Set

Due to the geometry of the shape and the order of tangency, four distinct types of points generically occur on the full SS [4, 15].

An A_1^2 point: the midpoint of circles tangent at two distinct points of the shape. These points are dense on the SS .

An A_3 point: the midpoint of a circle located at the evolute and tangent at the point of the shape with the local extremal curvature. The endpoint of a branch of the SS .

An A_1A_2 point: the midpoint of a circle tangent at two distinct points of the shape but located at the evolute. A turning point on the SS .

An A_1^3 point: the midpoint of one circle tangent at three distinct points of the shape. An intersection of three branches of the SS .

An A_1^2/A_1^2 point: the midpoints of two circles with different radii coincide and two branches of the SS intersect.

3.2.3 pre-Symmetry Set

The pre- SS is obtained by visualizing the Symmetry Set in parameter space, so essentially it is visualizing the zero crossings of $(p_i - p_j) \cdot (\mathcal{N}_i \pm \mathcal{N}_j)$. This is done in Figure 3.3. On the axis one finds the parameters p_i and p_j . The black curved lines represent the zero crossings.

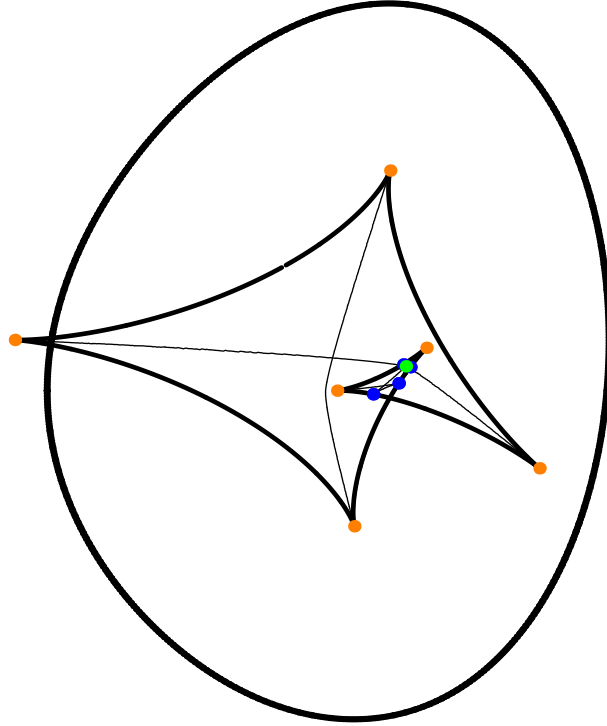


Figure 3.2: A shape (thickest), its evolute (thick) and the \mathcal{SS} with special points

Firstly, it needs to be remarked that the diagram repeats across its borders: the parameter moves along a closed curve. So the diagram represents a torus. Furthermore, the axis are to be identified, since they both relate to the same parameter along the shape. So the image is symmetric in the diagonal and the plot represents in fact a Möbius strip, with the diagonal as its boundary. In Figure 3.3, one can see two curves ranging over the entire domain and one closed loop.

3.2.4 Points on the Pre-Symmetry Set

Since curves in the pre- \mathcal{SS} generically don't intersect, one easily obtains separate branches. On these branches the points are classified as follows:

At A_3 points, one has $p_i = p_j$. They are located at the diagonal since they don't concern two different points on the shape.

At A_1A_2 points the \mathcal{SS} hits the evolute and is reflected. This implies that one of the two involved points is also reflected. The pre- \mathcal{SS} therefore has a horizontal or vertical tangent (identical due to symmetry in the diagonal).

At an A_1^3 point three parts of the \mathcal{SS} intersect. In the pre- \mathcal{SS} these points are detectable as the occurrence of the triple point sets (p_1, p_2) , (p_1, p_3) , and (p_2, p_3) (and, of course, the diagonal symmetric counterpart). This is visualized by the box-set in Figure 3.3.

All other points are A_1^2 points.

3.2.5 regularisation

If the shape is given as an unorganised point cloud, a parametrization is needed in order to use the above mentioned method. This can be obtained by taking one point and taking its closest neighbour from the remaining points. Next, the parametrization is regularized by convolution with a Gaussian kernel at a small scale. In this way also the derivatives at each point can be computed. An example is given in Figure 3.4. The left image shows

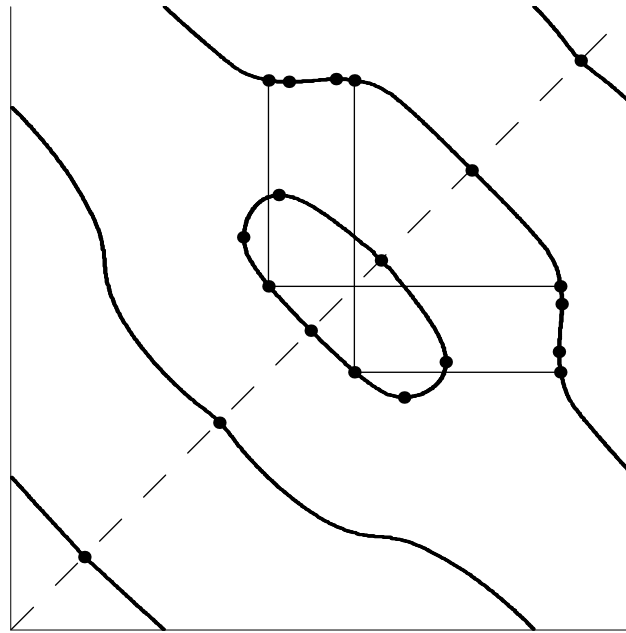


Figure 3.3: Pre- SS of the oval.

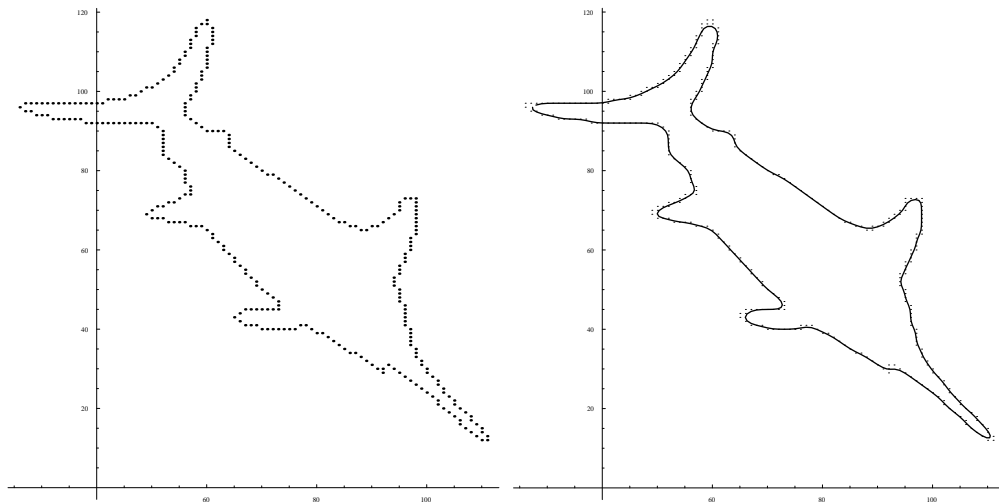


Figure 3.4: A pointcloud representing a fish and a regularized version of it.

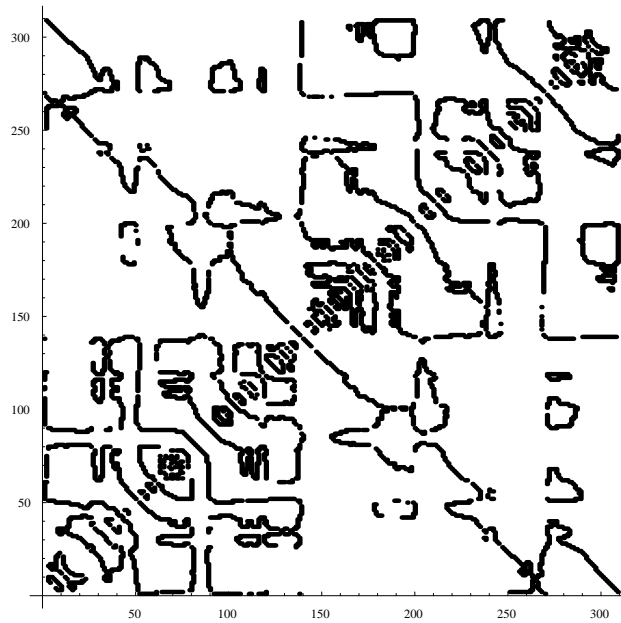


Figure 3.5: The pre-Symmetry of the regularized fish shape.

the points, while the right image shows the shape as it is obtained from these points.

The zero crossings of Eqs. 3.1 and 3.2 can easily be computed, yielding the pre-Symmetry Set for the fish shape of Figure 3.4 as shown in Figure 3.5.

3.3 Using the pre-ss

Given the pre-Symmetry Set and the Symmetry Set, one can find the Medial Axis by taking the maximal circles - by definition. They consist of those points (p_i, p_j) of the Symmetry Set where the radius is minimal for p_i with any point p_j that yields a zero crossing of Eq. 3.1. So for each horizontal (or equivalently, vertical) line in the pre-Symmetry Set we select a point p_i and find the points p_{j_k} where this line intersects with curves of the pre-Symmetry Set. For these k points we select the one with the smallest radius.

If we are only interested in the part of the skeleton that is inside the shape, we simply have to select the one with the largest negative value (i.e the negative value closest to zero), as the normals point outwards.

3.3.1 Branch types

Given the pre-Symmetry Set and the structure of the Medial Axis in general, we can note that the Medial Axis consists of two types of branches.

Firstly the branches with an endpoint, that end in a bifurcation point, or fork. That is, a part from an A_3 point, an endpoint, or local extremum of the curvature, to an A_1^3 point.

Secondly, there are parts going from a fork to a fork, or from an A_1^3 point to an A_1^3 point.

Now both A_3 and A_1^3 points can be found in the pre-Symmetry Set as points on the diagonal and as corners of the boxes, as in Figure 3.3.

A next observation for A_3 points yields, that these are local extrema of the curvature, and the reciproke of the radius. So only the negative local minima possibly count for the Medial Axis. Since they are on the diagonal in subsequential maximum - minimum order, they can be labelled subsequentially with odd and even numbers and only -say- odd numbers do have to be taken into account. So the Medial Axis in the pre-Symmetry Set contains at least a set of curve-parts through the diagonal.

Next, also fork-to-fork are (in almost all cases) present. They can be understood as the set of points (p_i, p_j) with i increasing and j decreasing along the shape that suddenly meet a third point p_k causing the combinations (p_i, p_j) , (p_i, p_k) , and (p_k, p_j) with equal radius. Increasing i and decreasing j now the skeleton is formed by the two parts derived from the combinations (p_i, p_{k_1}) and (p_{k_2}, p_j) , with i and k_2 increasing and j and k_2 decreasing. In the pre-Symmetry Set this is represented as a jump. Since all points of the shape contribute once to the Medial Axis, one of two essential loops of the pre-Symmetry Set contains fork-to-fork parts. This curve of the pre-Symmetry Set can be considered as the main skeleton axis

Finally, for Shock Graph applications, also necks are considered: these are the circles with locally maximal or minimal radii when moving along the Medial Axis. In the pre-Symmetry Set they are straightforwardly obtained as the points that have parallel tangent, i.e. Symmetry Set points that are also Anti-Symmetry Set points.

3.3.2 Algorithm

The construction of the skeleton thus takes place by taking the minimal radius, selecting the points (p_i, p_j) contributing to this radius, and repeating this for the remainder of the points.

1. Solve Eqs. 3.1 and 3.1 for all points p_i on the shape, yielding triplets $q_k = (p_i, p_j, r(p_i, p_j))$. Note that each p_i and p_j can occur multiple times.
2. Set $Q = \{q_k \mid r < 0\}$: select only the interior points.
3. Set $MA = \emptyset$
4. Find $R = r_{\max} \in Q$ and $p_R = (p_\alpha, p_\beta, R)$.
5. Add p_R to MA
6. Remove all points in Q containing p_α and p_β .
7. Go back to 4 until Q is empty.

3.4 Example

For the fish shape, the parts of the Medial Axis in the pre-Symmetry Set are shown in Figure 3.6. Next, the fish with its Medial Axis is shown in Figure 3.7. The distinct parts of the Medial Axis are labelled, with numbers for end-point-to-fork branches, and capitals for fork-to-fork branches. The point labelling starts most left and anti-clock wise. Therefore the left tailbranch gets label 1.

For a detailed discussion on the branches, consider also Figure 3.8, where the Medial Axis is shown in the pre-Symmetry Set space.

Firstly, note that the end-point-to-fork branches all intersect the diagonal. They are numbered according to the point labelling along the shape, so in simple increasing order. Since always two different points are found, there are no pairs (p_i, p_i) , but only pairs $(p_i + 1, p_i)$ and $(p_i, p_i + 1)$ that are part of diagonal intersecting curves. Therefore, the first branch is only visible top left and (connected to) bottom right. The branches 5 and 7 each contain 1 point, and especially branch 7 is hardly visible. It almost coincides with the other points.

Secondly, the inner fork-to-fork branches are - in this case - all located on the essential curve. This curve connects the left tail (branch 1) to the nose (branch 6). This can be regarded as the main axes of the fish.

The traversal along the branches can be traced in both Figures. Starting at the nose, branch 6, at a certain moment branch 5 comes in, forming a fork with branch A. This branch meets branch 7 and branch B. The latter meets branches 4 and the very small branch C, that immediately meets branch 8 and branch D. In Figure 3.7 these combinations are rather obvious, in Figure 3.8 they can be traced by drawing the boxes that define the A_1^3 points. In this Figure, one can distinguish between left and right parts of the shape. Firstly, the beginpoint of the parameterization can be chosen such, that it is located at the end of an essential loop, just as in this example. This is due to the fact that the parameterization is rotationally invariant. Therefore, one can define

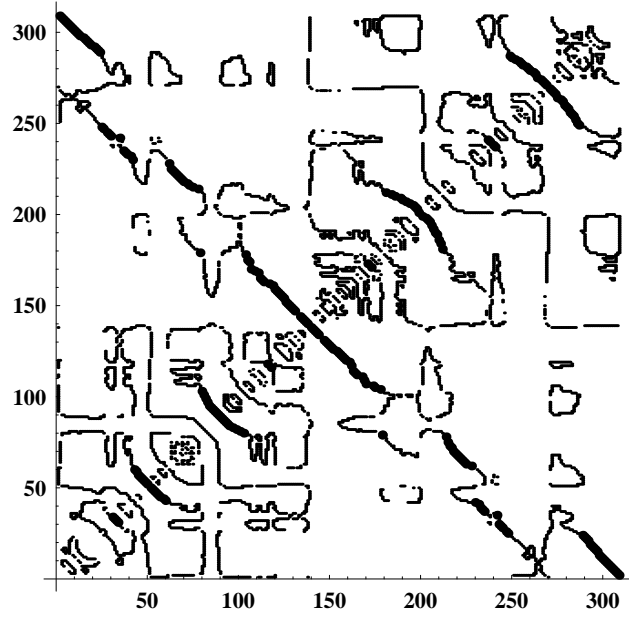


Figure 3.6: The pre-Symmetry Set of the fish shape with the Medial Axis part in thick.

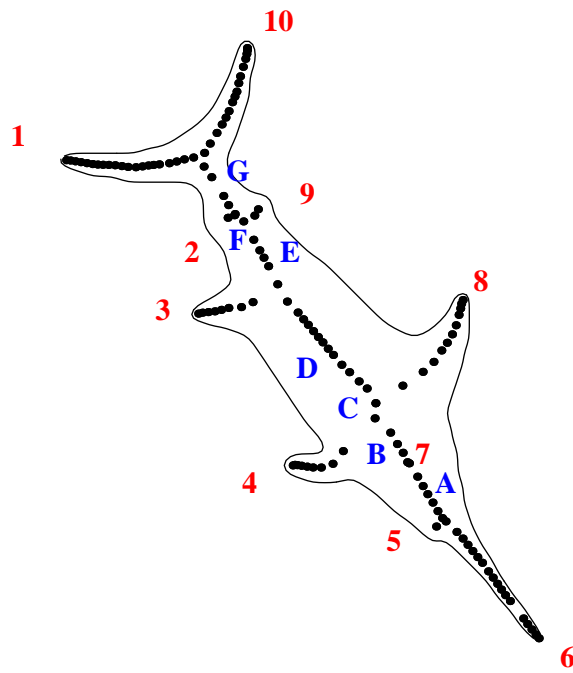


Figure 3.7: Medial Axis of the fish, with labels (see text)

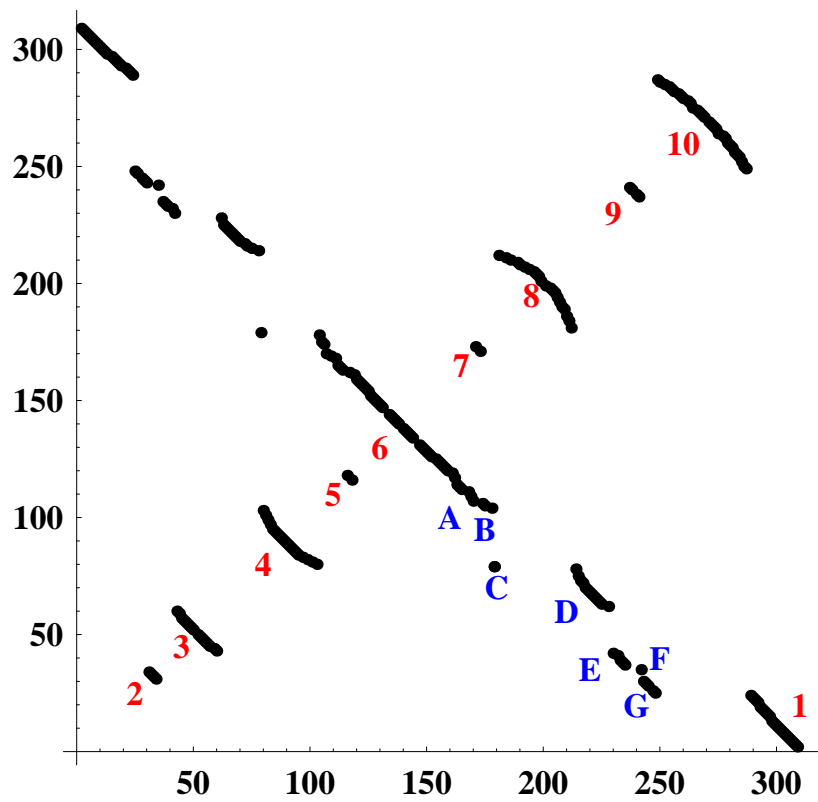


Figure 3.8: Medial Axis in the Pre-Symmetry Set of the fish, with labels (see text).

an "anti-diagonal", by the points (p_i, p_{n-i}) , with n the number of points. Along this anti-diagonal the main medial axis will approximately be located. Points under or left of this anti-diagonal lie on the same side (say left) of the main medial axis, vice versa. In the example, one can verify that the branches 2 to 5 are indeed on the left, while 7 to 10 are on the right

Note that in this example the fork-to-fork branches are aligned. Obviously, this need not be the case in general.

3.5 Summary and Conclusions

In this paper we presented a method to extract the skeleton, or Medial Axis, in a novel way. The method is based on the Symmetry Set and used the fact that the Medial Axis is a subset of the Symmetry Set. It boils down to select those Symmetry Set points that give rise to maximal circles - which is exactly the definition of the Medial Axis as subset of the Symmetry Set. By construction, for each pair of points we find exactly one skeleton point, so the number of skeleton points is approximately half of the number of shape points. The normal vectors required for the algorithm are obtained by a small regularization of the shape, while the computation doesn't introduce new (interpolated) points. Therefore, the result will be a collection of point. For visualization or other post-processing purposes, the skeleton can of course be smoothed, connected (which is fairly trivial using the branches of the pre-symmetry Set) or complemented with additional points.

Chapter 4

The Structure of Shapes

Abstract

Images simplify due to the heat equation, yielding a Gaussian scale space image. Shapes simplify similarly due to the intrinsic heat equation and form a scale space shape. For images, the resulting structure is known to embed a hierarchical structure, based on singularity theory, and investigated to some extent. Shapes, when simplified under certain conditions, also undergo specific singularities. In this paper we present the general framework of a shape scale space, based on a Medial Axis carrying structure called Symmetry Set.

4.1 introduction

Among attempts to represent shapes differently, the skeleton [2], or medial axis, takes an important role. It is defined as the closure of the centers of maximal circles tangent to the shape at at least two points. Popular: the set of points that have the same minimal distance to at least two points on the shape. Modifications of the skeleton made it more stable [36]. The Shock Graph approach [41] incorporates distance information at some points. and recently, promising results were presented on matching of these descriptions [35] using the possible changes of the Shock Graphs.

The medial axis is a subset of the symmetry set [4]. Changes of this set (transitions, singularities) [3] are directly responsible for changes of the medial axis [15]. The symmetry set can easily be computed and appears to be able to be represented as a string-like data structure that allows operations with very low computational complexity [24, 28]. An extra advantage is that all extremal curvature points are taken into account.

All these methods start from the given shape and do not take into account the scale as a free parameter. In general, the radius of the circle is considered as scale, but the radius is introduced by definition of the medial axis.

A solution to the problem of scale comes from mathematics. In order to be able to treat discontinuous data in a continuous way, one needs regularize the data or, equivalently, to use test-functions [38], or perform a local integration at observation points. One suitable testfunction is the Gaussian filter [9, 10]. By keeping the variance of the filter a free parameter, one obtains a multiscale extension of the original image, as originally proposed by Koenderink [22], and followed by many others, see e.g. [8, 18, 29, 47, 19, 33, 21, 17]. Investigation of the deep structure, i.e. the image at all scales simultaneously, led, among other things, to the discovery of a topological hierarchy within the image extended with a scale variable [23].

This idea can be directly transferred to shapes. For shapes, the intrinsic heat equation is the Mean Curvature Motion, see e.g. [5]. An example is shown in Figure 4.3. The changes in the Symmetry Set (the local situations) are theoretically known [3], also under the influence of Mean Curvature Motion [45].

In this paper the Symmetry Set method is embedded in a multiscale context - just as zero crossings of the curvature in the Curvature Scale Space method. This novel approach creates a multiscale symmetry set that reveals a hierarchical simplification of the Symmetry Set as the scale increases.

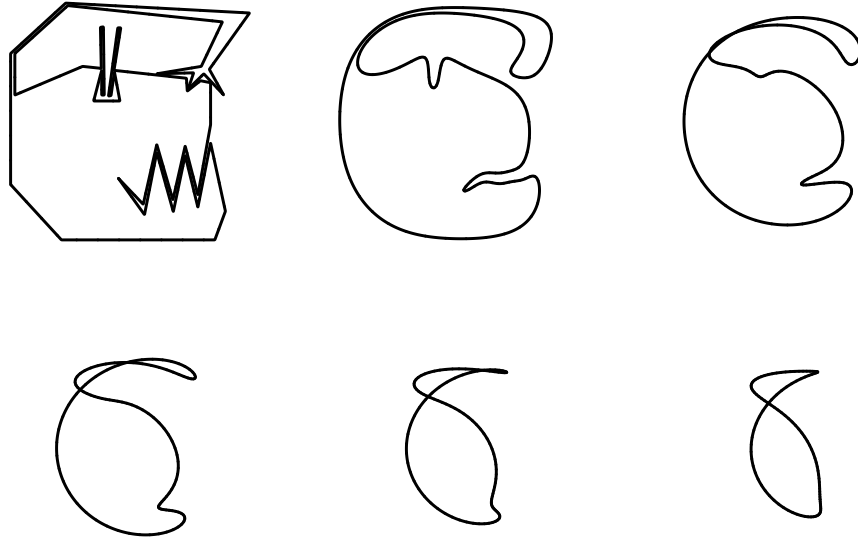


Figure 4.1: Applying Gaussian blurring on the $(x(t), y(t))$ coordinates separately doesn't equal applying Mean Curvature Motion, but can cause selfintersections and cusp points. The example is taken from Cao [5].

4.2 Background

We firstly provide some background theory regarding shapes, their evolution, and their symmetry set-based representations.

4.2.1 Shapes

Let $\mathcal{S}(x, y) = \{(x, y) | L(x, y) = 0\}$ denote a closed 2D shape. Then $\mathcal{N}(x, y) = (L_x, L_y)(L_x^2 + L_y^2)^{-1/2}$ denotes its unit normal vector, and $\kappa(x, y) = -(L_x^2 L_{yy} - 2L_x L_y L_{xy} + L_y^2 L_{xx})(L_x^2 + L_y^2)^{-3/2}$ its curvature. The evolute $\mathcal{E}(t)$ is given by the set $\mathcal{S} + \mathcal{N}/\kappa$. Even if the curve is smooth and differentiable, the evolute contains non-smooth and non-differentiable points, viz. those where the curvature is zero or takes a local extremum, respectively.

4.2.2 Evolution

Let $S(x(p), y(p))$ be a curve given in its parameterized coordinates, and p taken on the unit circle S^1 . Then the simplest way of regularizing the curve is by convolving it with the simplest smoothing kernel, a Gaussian (see Cao [5] for more details). Then the heat equation is solved for each of the coordinates:

$$\frac{\partial x}{\partial t} = \frac{\partial^2 x}{\partial p^2}, \quad \frac{\partial y}{\partial t} = \frac{\partial^2 y}{\partial p^2}.$$

Now the coordinates $x(p, t)$ and $y(p, t)$ are smooth, but the curve may become non-smooth, see Figure 4.1

The reason for this is the fact that the parametrization parameter p describes a curve that shrinks as the scale increases. To overcome aforementioned problem, the curve needs a renormalization s_σ at every scale σ , as proposed by Mokhtarian and Mackworth [32]. Solving the heat equation between two infinitesimal close instances (and renormalizations) yields

$$\frac{\partial x}{\partial t} = \frac{\partial^2 x}{\partial s^2}, \quad \frac{\partial y}{\partial t} = \frac{\partial^2 y}{\partial s^2}.$$

called the intrinsic heat equation. The parameter s is also called the arc-length. This gives the mean curvature motion:

$$\frac{\partial C}{\partial t} = \frac{\partial^2 C}{\partial s^2} = \kappa N$$

where κ is the curvature and N the unit length normal. Note that in this equation the arc-length s depends on t , so the equation is non-linear. Each point on the curve moves in the direction of the normal, proportional to the curvature. Some results of motion are due to Gage and Hamilton [11] and Grayson [16]: a curve becomes convex and shrinks to a point at $t = T$, $T = A_0/2\pi$, A_0 the area enclosed originally by the curve. The curve will stay smooth during evolution (no selfintersections or cusp points). This compares to the properties of Gaussian blurring for images.

When the curve is considered as a level line (an isophote) of an image L , κN equals $\|\nabla L\|\nabla \cdot (\nabla L/\|\nabla L\|)$, or in short gauge coordinates, L_{vv} : the second order derivative in the direction tangential to the isophote. The image evolution is called Euclidean shortening flow.

When the zero-crossings of the curvature over scale are traced, one applies a Curvature Scale Space [32]. This appeared to be a powerful and fast shape description that is taken into the MPEG7 Standardization [31].

4.2.3 Symmetry Set

The Medial Axis (\mathcal{MA}) of a shape is defined as the closure of the set of centers of circles that are tangent to the shape at least two points and that contain no other tangent circles: the are so-called maximal circles. The Symmetry Set \mathcal{SS} is defined as the closure of the set of centers of circles that are tangent to the shape at least two points [4, 3, 13, 12]. Obviously, the \mathcal{MA} is a subset of the \mathcal{SS} [12].

To calculate these sets from above definition, the following procedure can be used: Let a circle with unknown location be tangent to the shape at two points. Then its center can be found by using the normal vectors at these points: it is located at the position of each point minus the radius of the circle times the normal vector at each point. To find these two points, the location of the center and the radius, do the following: Given two vectors p_i and p_j (right, with $i = 1$ and $j = 2$) pointing at two locations at the shape, construct the difference vector $p_i - p_j$. Given the two unit normal vectors N_i and N_j at these locations, construct the vector $N_i + N_j$. If the two constructed vectors are non-zero and perpendicular,

$$(p_i - p_j) \cdot (N_i + N_j) = 0, \quad (4.1)$$

the two locations give rise to a tangent circle. The radius r and the center of the circle are given by

$$p_i - rN_i = p_j - rN_j. \quad (4.2)$$

In Figure 4.2a, the shape is given by the oval. Inside a circle is tangent to it at two locations, so the *unit* normals \mathcal{N}_1 and \mathcal{N}_2 are equal for the shape and the circle. The centre of the circle is found by multiplying minus the radius r with the normals. Note that this is also a \mathcal{MA} point. Next, also outside a circle is tangent to the shape at two locations, where the unit normals \mathcal{N}_1 and \mathcal{N}_4 are equal for the shape and the circle. From this image it follows immediately that a point on the shape relates to at least two points on the \mathcal{SS} , in contrast with the \mathcal{MA} . Changes in the shape yield changes in the symmetry set and are well-known [3]. The symmetry set can be represented as a string structure (while the MA requires a graph), whose changes are directly inherited from the symmetry set [28].

4.2.4 pre-Symmetry Set

The pre-Symmetry Set is defined as the Symmetry Set in parameter space: instead of the centers of the circles defining the Symmetry Set, the points on the shape where these circles are tangent, are taken. This yields the same (data), but in this case the representation is clearer [28, 26]. The pre-Symmetry Set representation of Figure 4.3 is shown in Figure 4.4. In a pre-Symmetry Set diagram, the two axes represent points on the shape. If two points p_i and p_j give rise to a Symmetry Set point, the corresponding points (p_i, p_j) and, due to symmetry, (p_j, p_i) are marked in the diagram. The diagram shows curves that continue along the boundaries. Each curve represents a distinct part of the Symmetry Set.

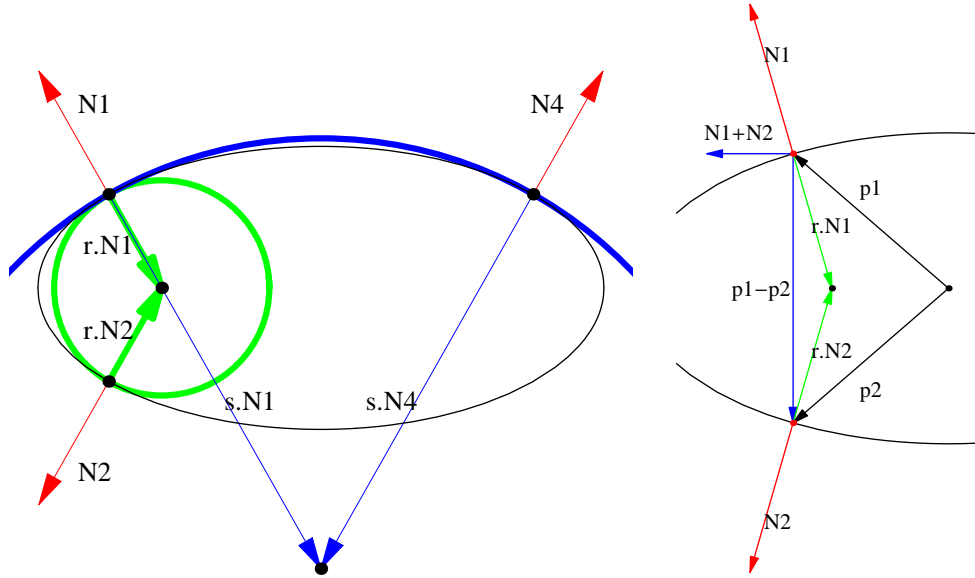


Figure 4.2: a) Circles tangent to a shape b) Computing the Symmetry Set (see text).

On the pre-Symmetry Set, the changes of the structure can be detected as well, they can even be labeled with relevance with respect to changes in number of elements (curves), smoothness of elements, swapping of branches of two curves, and changes in the number of special points related to the junctions of the skeleton [27, 25].

4.3 Representation

In this section we elaborate on the pre- SS representation, give properties of it and propose a novel representation with properties that are inherited from the pre- SS .

4.3.1 Properties of the pre-Symmetry Set

An intersection of curves in the pre- SS is due to a swap-transition. The endpoints of the SS are located at the diagonal of the pre- SS . They relate to points of extremal curvature on the shape. The points can be sequentially numbered. Along the diagonal, the type of extremum alternates, just as along the shape. So without loss of generality we may think of minima as odd numbered intersections and maxima as even ones. For closed curves, the pre- SS contains two essential loops, loops that range over the complete parameter domain. They connect points of equal type of curvature extremum: one connecting two even intersections, one connecting two odd ones. All other curves connect curvature extrema of different types (even-odd intersections).

Created or annihilated curves always involve an even-odd couple. Swappings always involve an even-odd couple and an arbitrary couple, and must result in an even-odd and an arbitrary one. For example two even-odd couples (say 1-2 and 3-4) result in two even-odd couples (1-4 and 2-3), and an even-odd and an even-even couple (say 3-4 and 2-6) result in an even-odd and an even-even couple (2-3 and 4-6). Note that the non-intersecting property puts restrictions on the possibilities. In the first example, the couples 1-3 and 2-4 are forbidden, since these curves have to intersect in the pre- SS . The same holds for the couple 3-6 and 2-4 in the second example. There can be only two essential loops. One can think of them as the probing of the shape with two circles, one inside the shape and one outside, or alternatively, one loop (axis of symmetry) for each dimension of space in which the shape is embedded.

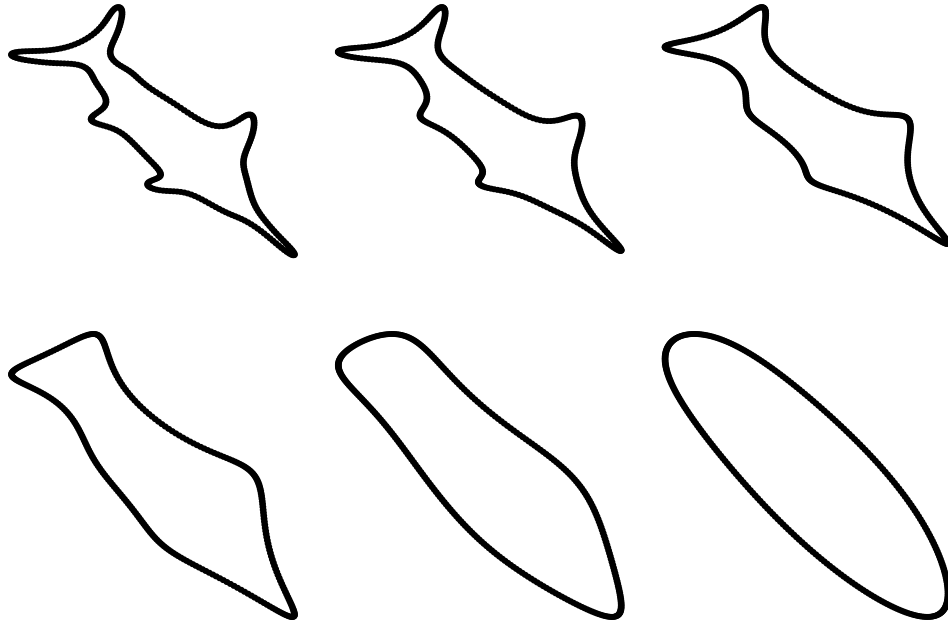


Figure 4.3: The fish shape top left transforms into a circle under influence of Mean Curvature Motion

Also non-diagonal intersecting closed curves exist, so-called moths. Since they are only relevant when they interact in a swapping event - which basically makes another curve longer, we will ignore them in the latter.

4.3.2 Gauss diagram

The pre-Symmetry Set has a dual type of representation, viz. that of a circle with chords. The circle represents the closed curve and is obtained by taking the diagonal in the pre-Symmetry Set, connecting both ends. The cords represent the distinct parts of the Symmetry Set, the curves in the pre-Symmetry Set. Just as the pre-Symmetry Set diagram, this chord diagram has special properties. It is very alike the Gauss diagram known from Knot theory [37, 46]. The most evident property is the fact that exactly two cords are intersecting, dividing the circle in four quarter. These cords represent the two essential loops. Each quarter contains nested or sequential cords. The moth circles appear as small circles within a quarter.

Transitions of the Gauss diagram relate directly to those of the pre- \mathcal{SS} : we can have annihilations (creations) of cords as their length tends to (start from) a point on the circle. And we can have swappings of cords. Note that we can add extra information on the cord.

4.4 Multi-scale shape hierarchy

Given a set of data points of a shape, regularization of these points is needed in order to obtain more detailed information with respect to their location and their derivatives. A small Gaussian kernel applied to the coordinates can do this. However, why choose one specific scale? A more thrustworthy way is choosing no a priori scale. As discussed in Section 4.2, a Gaussian is not the best kernel to convolve with. For shapes the intrinsic heat equation is appropriate. Figure 4.3 shows the fish image under the influence of mean curvature motion.

For each scale the pre- \mathcal{SS} can be calculated. This yields surfaces in the pre- \mathcal{SS} scale space. For large scales two sheets remain, representing the essential loops. The transitions of the \mathcal{SS} under MCM have been described by Teixeira [45]. The only allowed transitions are annihilations, swappings, and smooting and curving of curves. Annihilations imply that closed loops of the pre- \mathcal{SS} shrick to circular structures and disappear. The manifolds are cones. Swappings imply that two manifolds are connected at one point, the "swapping-

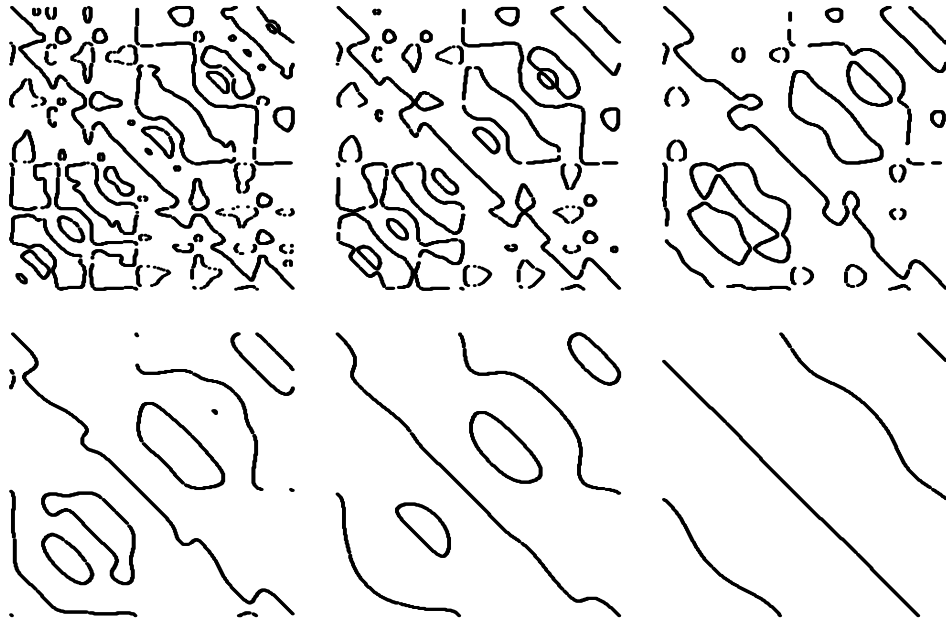


Figure 4.4: The pre-Symmetry Set of the fish shape transforms to four parallel lines (two essential loops) under influence of Mean Curvature Motion.

transition". Smoothing and curving of curves means that manifolds can be waving-like. The pre-SS representing the simplifying fish sequence is shown in Figure 4.4

4.4.1 Comparison with Curvature Scale Space

Although the concept of Curvature Scale Space (CSS) also uses the idea of evolution due to Mean Curvature Motion, there are significant differences. CSS investigates the zero crossings of the curvature over scale and is not related to medial axis methods. For instance, all convex shapes have the same (zero) Curvature Scale Space representation. Here zero crossings of derivative of curvature are considered (i.e. the extrema of κ) instead of zerocrossings of the curvature itself.

In Figure 4.6 the CSS of the fish is shown on the left. Note that all branches end at a certain scale, when the shape becomes convex. In the middle, the extrema of the curvature are shown. Now exactly 4 branches remain, resembling the 4 extremal curvatures of an oval. On the right these curves are shown as function of their spatial and scale positions.

The essential difference is that these curves show the connections with respect to their annihilations, while the Symmetry Set connections are related to all their intermediate connections, which may - and almost always do - change.

4.4.2 Gauss Diagrams under Mean Curvature Motion

Next, also the Gauss diagrams change under MCM. They inherit the transitions from the pre-SS scale space. They are: annihilations of cords, swapping of cords and changing of labels on a cord. The diagrams representing the simplifying fish sequence is shown in Figure 4.7.

For all possible shapes we can construct a space of gauss diagrams. Given the simplification of structure as scale increases, we can construct a directionality into this space, as shown in Figure 4.8. At the top the simplest shape, an ellipsis, is represented by two intersection cords. At each subsequent level, a cord is added. At a specific level, the positions of cords can change due to swappings.

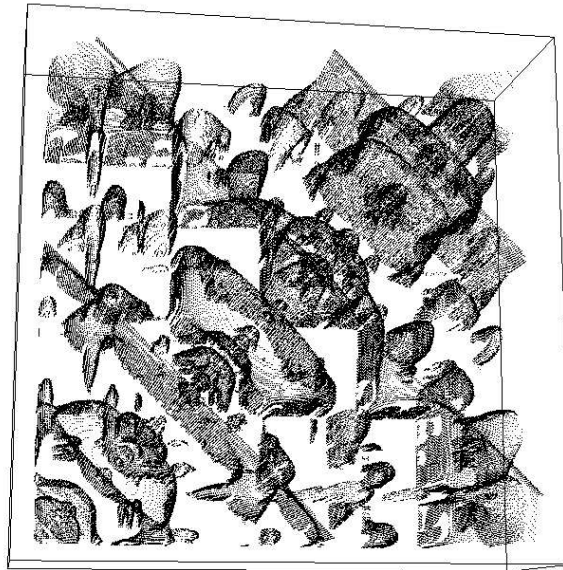


Figure 4.5: The pre-Symmetry Set of the fish shape transforms to four parallel lines (two essential loops) under influence of Mean Curvature Motion.

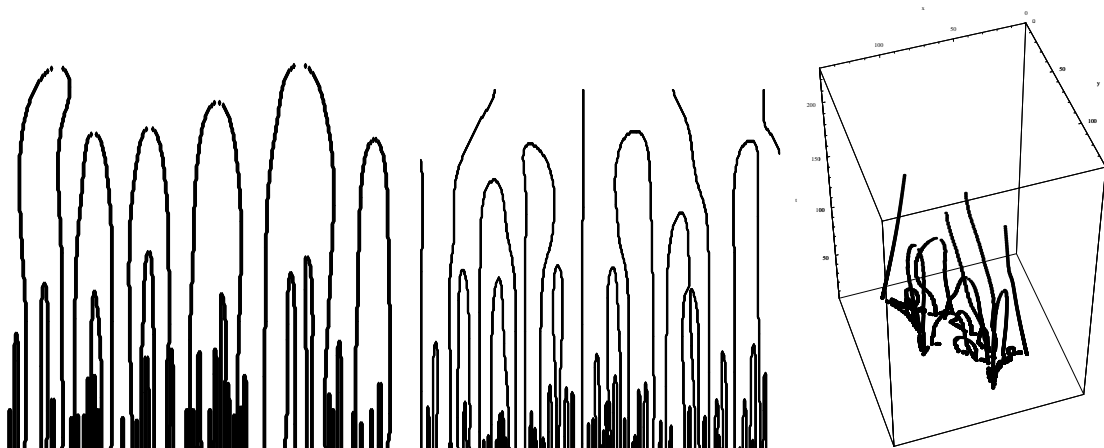


Figure 4.6: Left: CSS of the fish. Middle: evolution of the extrema of the curvature of the fish. Right: Position of the curvature extrema of the fish in scale space.

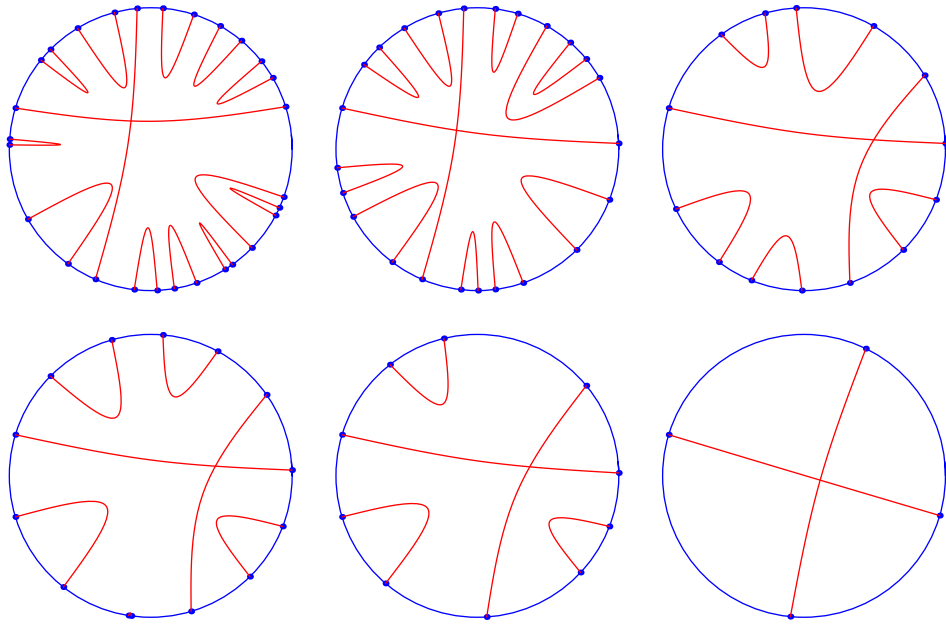


Figure 4.7: The Gauss diagrams of the fish shape transforms into a circle with two intersecting chords under influence of Mean Curvature Motion.

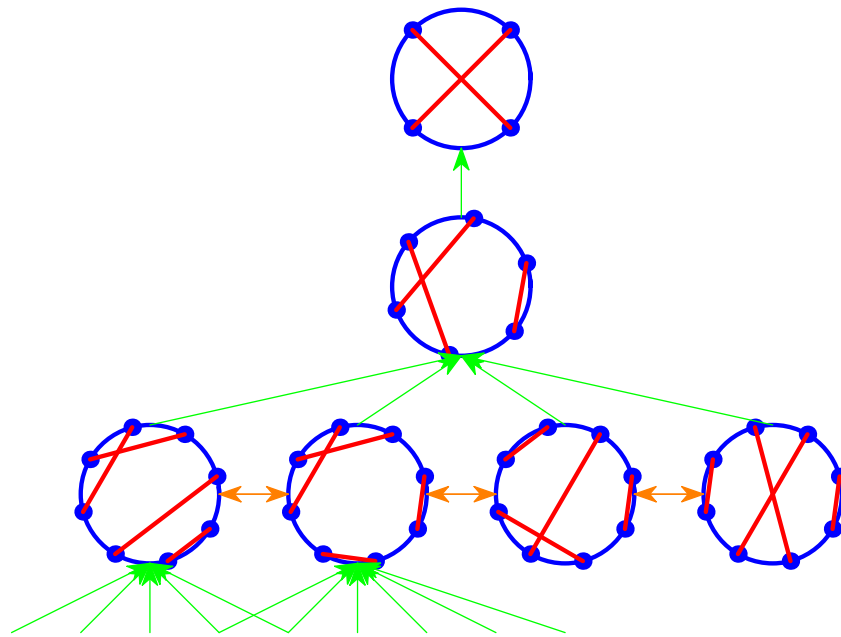


Figure 4.8: The Gauss diagrams under influence of Mean Curvature Motion form a hierarchy. The horizontal level represents the number of cords (of A_3 points, or extrema of curvature). They change under A_4 transitions in a simplifying manner: cords disappear. At the horizontal levels cords swap due to A_2^2 transitions. A further refinement can be achieved by adding the $A_1 A_2$ along the cords.

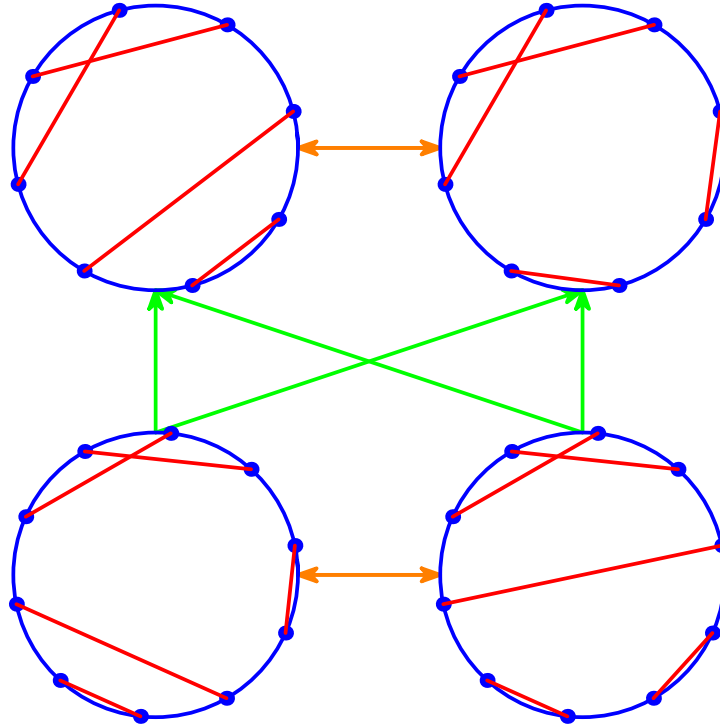


Figure 4.9: The state space of Gauss diagrams is a directed graph. Simplification can be achieved in different ways,

One thus obtains hierarchical metameric classes. Obviously, adding information to the cords enlarges the possible diagrams and decreases the size of the class. The swapping is not the only reason that the graph is not a tree. Also the disappearing of cords can relate to causes a childnode to be possibly related to multiple parents, in contrast to trees, as shown in Figure 4.9.

At a certain level, two subsequent swappings can as well take place in one swap, see Figure 4.10.

Given an arbitrary closed non-intersecting curve, applying MCM yields a convex shape shrinking to a point at a sufficiently large scale. So the accompanying Gauss diagrams are related to a path through the space of all possible diagrams. Each shape will have its own path, and “more of less” similar shapes will have paths that coincide at some stage. So the difference of the shapes can be expressed as the difference in paths.

4.5 Conclusions

In this paper we presented a truly multiscale hierarchy for shapes, based on the symmetry set. The multi scale hierarchy is obtained by evolving the shape and its symmetry set under mean curvature motion, the intrinsic heat equation for shapes. As data structure the pre-symmetry set, visualized in a Gauss diagram is taken. This allows one to map the data on a circle, and effectively represent the multiscale representation as a cylinder with connected points at each scale, i.e. a cylinder with sheets. Changes as scale increases are well-defined and known, which makes this structure suitable as a descriptive space for shapes. Since all shapes converge to the same structure, difference in shapes can be expressed in difference of convergence paths.

Acknowledgements

The authors thank Prof. Giblin from Liverpool University and Prof. Siersma from Utrecht University for fruitful discussions.

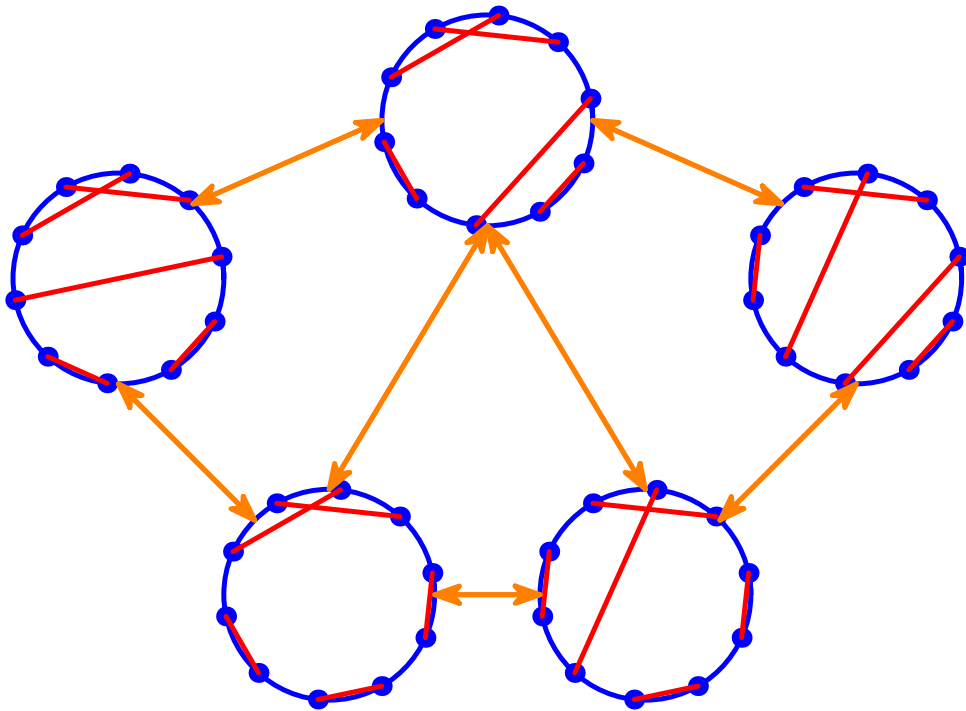


Figure 4.10: At a specific level multiple A_2^2 transitions are possible for changing the cords of the Gauss diagrams.

Bibliography

- [1] V. Bafna, S. S. Muthukrishnan, and R. Ravi. Computing similarity between rna strings. In *Proceedings of the Sixth Symposium on Combinatorial Pattern Matching (CPM'95)*, pages 1–16, 1995. LNCS 937.
- [2] H. Blum. Biological shape and visual science (part i). *Journal of Theoretical Biology*, 38:205–287, 1973.
- [3] J. W. Bruce and P. J. Giblin. Growth, motion and 1-parameter families of symmetry sets. *Proceedings of the Royal Society of Edinburgh*, 104(A):179–204, 1986.
- [4] J. W. Bruce, P. J. Giblin, and C. Gibson. Symmetry sets. *Proceedings of the Royal Society of Edinburgh*, 101(A):163–186, 1985.
- [5] F. Cao. *Geometric Curve Evolution and Image Processing*, volume 1805 of *Lecture Notes in Mathematics*. Springer Verlag, 2003.
- [6] E. S. Deutsch. Thinning algorithms on rectangular, hexagonal, and triangular arrays. *Communications of the ACM*, 15(9):827–837, 1972.
- [7] P. Dimitrov, J.N. Damon, and K. Siddiqi. Flux invariants for shape. *Proceedings of the IEEE Conference on Computer Vision and Pattern Recognition, 2003.*, 1:835–841, 2003.
- [8] L. M. J. Florack. *Image Structure*, volume 10 of *Computational Imaging and Vision Series*. Kluwer Academic Publishers, Dordrecht, The Netherlands, 1997.
- [9] L. M. J. Florack, B. M. ter Haar Romeny, J. J. Koenderink, and M. A. Viergever. Scale and the differential structure of images. *Image and Vision Computing*, 10(6):376–388, July/August 1992.
- [10] L. M. J. Florack, B. M. ter Haar Romeny, J. J. Koenderink, and M. A. Viergever. Linear scale-space. *Journal of Mathematical Imaging and Vision*, 4(4):325–351, 1994.
- [11] M. Gage and R. S. Hamilton. The heat equation shrinking convex plane curves. *J. Differential Geom.*, 23(1):69–96, 1986.
- [12] P. J. Giblin and B. B. Kimia. On the intrinsic reconstruction of shape from its symmetries. In *IEEE Conference on Computer Vision and Pattern Recognition, 1999*, pages 79–84, 1999.
- [13] P. J. Giblin and B. B. Kimia. On the local form and transitions of symmetry sets, medial axes, and shocks. In *Proceedings of the 7th International Conference on Computer Vision (1999)*, pages 385–391, 1999.
- [14] P. J. Giblin and B. B. Kimia. On the intrinsic reconstruction of shape from its symmetries. *IEEE Transactions on Pattern Analysis and Machine Intelligence*, 25(7):895–911, July 2003.
- [15] P. J. Giblin and B. B. Kimia. On the local form and transitions of symmetry sets, medial axes, and shocks. *International Journal of Computer Vision*, 54(1/2):143–156, 2003.
- [16] Matthew A. Grayson. The heat equation shrinks embedded plane curves to round points. *J. Differential Geom.*, 26(2):285–314, 1987.
- [17] L.D. Griffin and M. Lillholm, editors. *Scale Space Methods in Computer Vision*, volume 2695 of *Lecture Notes in Computer Science*. Springer -Verlag, Berlin Heidelberg, 2003.
- [18] B. M. ter Haar Romeny. *Front-end vision and multi-scale image analysis*, volume 27 of *Computational Imaging and Vision Series*. Kluwer Academic Publishers, Dordrecht, The Netherlands, 2003.
- [19] B. M. ter Haar Romeny, L. M. J. Florack, J. J. Koenderink, and M. A. Viergever, editors. *Scale-Space Theory in Computer Vision: Proceedings of the First International Conference, Scale-Space'97, Utrecht, The Netherlands*, volume 1252 of *Lecture Notes in Computer Science*. Springer-Verlag, Berlin, July 1997.
- [20] M. Hisada, A. G. Belyaev, and T. L. Kunii. Towards a singularity-based shape language: ridges, ravines, and skeletons for polygonal surfaces. *Soft Computing*, 7(1):45–52, 2002.

- [21] M. Kerckhove, editor. *Scale-Space and Morphology in Computer Vision*, volume 2106 of *Lecture Notes in Computer Science*. Springer -Verlag, Berlin Heidelberg, 2001.
- [22] J. J. Koenderink. The structure of images. *Biological Cybernetics*, 50:363–370, 1984.
- [23] A. Kuijper. *The Deep Structure of Gaussian Scale Space Images*. PhD thesis, Utrecht University, 2002.
- [24] A. Kuijper. Computing symmetry sets from 2D shapes. Technical Report TR-2003-36, IT University of Copenhagen, 2003. ISBN 87-7949-049-2, TR-2003-36. <http://www.itu.dk/pub/Reports/ITU-TR-2003-36.pdf>.
- [25] A. Kuijper. On data structures from symmetry sets of 2D shapes. Technical Report TR-2004-47, IT University of Copenhagen, 2004. ISBN 87-7949-069-7, <http://www.itu.dk/pub/Reports/ITU-TR-2004-47.pdf>.
- [26] A. Kuijper and O.F. Olsen. On extending symmetry sets for 2D shapes. In *Proceedings of the Joint IAPR International Workshops on Syntactical and Structural Pattern Recognition (SSPR 2004) and Statistical Pattern Recognition (SPR 2004) Lisbon, Portugal, August 18-20, 2004*, pages 512–520, 2004. LNCS 3138.
- [27] A. Kuijper and O.F. Olsen. Transitions of the pre-symmetry set. In *Proceedings of the 17th International Conference on Pattern Recognition - ICPR 2004, Cambridge, UK, 23-26 August, 2004*, volume III, pages 190–193, 2004.
- [28] A. Kuijper, O.F. Olsen, P.J. Giblin, Ph. Bille, and M. Nielsen. From a 2D shape to a string structure using the symmetry set. In *Proceedings of the 8th European Conference on Computer Vision - ECCV 2004, Part II (Prague, Czech Republic, May 11-14, 2004)*, volume II, pages 313–326, 2004. LNCS 3022.
- [29] T. Lindeberg. *Scale-Space Theory in Computer Vision*. The Kluwer International Series in Engineering and Computer Science. Kluwer Academic Publishers, 1994.
- [30] R. Malladi, J.A. Sethian, and B.C. Vemuri. Shape modeling with front propagation: a level set approach. *IEEE Transactions on Pattern Analysis and Machine Intelligence*, 17(2):158–175, 1995.
- [31] F. Mokhtarian and M. Z. Bober. *Curvature Scale Space Representation: Theory, Applications, & Mpeg-7 Standardization*, volume 25 of *Computational Imaging and Vision Series*. Kluwer Academic Publishers, Dordrecht, The Netherlands, 2003.
- [32] Farzin Mokhtarian and Alan K. Mackworth. A theory of multiscale, curvature-based shape representation for planar curves. *IEEE Transactions on Pattern Analysis and Machine Intelligence*, 14(8):789–805, 1992.
- [33] M. Nielsen, P. Johansen, O. Fogh Olsen, and J. Weickert, editors. *Scale-Space Theories in Computer Vision*, volume 1682 of *Lecture Notes in Computer Science*. Springer -Verlag, Berlin Heidelberg, 1999.
- [34] R. L. Ogniewicz and O. Kubler. Hierarchic voronoi skeletons. *Pattern Recognition*, 28(3):343–359, 1995.
- [35] M. Pelillo, K. Siddiqi, and S. Zucker. Matching hierarchical structures using association graphs. *IEEE Transactions on Pattern Analysis and Machine Intelligence*, 21(11):1105–1120, 1999.
- [36] S.M. Pizer, K. Siddiqi, G. Székely, J.N. Damon, and S.W. Zucker. Multiscale medial loci and their properties. *International Journal of Computer Vision*, 55(2/3):155–179, 2003.
- [37] M. Polyak and O. Viro. Gauss diagram formulas for vassiliev invariants. *International Mathematical Research Notes*, 11:445–454, 1994.
- [38] L. Schwartz. *Théorie des Distributions*, volume I, II of *Actualités scientifiques et industrielles; 1091,1122*. Publications de l’Institut de Mathématique de l’Université de Strasbourg, Paris, 1950–1951.
- [39] T.B. Sebastian, P.N. Klein, and B. B. Kimia. Recognition of shapes by editing shock graphs. In *Proceedings of the 8th International Conference on Computer Vision (2001)*, pages 755–762, 2001.
- [40] K. Siddiqi, S. Bouix, A. Tannenbaum, and S. W. Zucker. The Hamilton-Jacobi skeleton. In *Proceedings of the 78th International Conference on Computer Vision (1999)*, pages 828–834, 1999.
- [41] K. Siddiqi, A. Shokoufandeh, S. Dickinson, and S. Zucker. Shock graphs and shape matching. *International Journal of Computer Vision*, 30:1–22, 1999.
- [42] Kaleem Siddiqi, Sylvain Bouix, Allen Tannenbaum, and Steven W. Zucker. Hamilton-jacobi skeletons. *International Journal of Computer Vision*, 48(3):215–231, 2002.
- [43] Dirk Siersma. Properties of conflict sets in the plane. In *Geometry and Topology of Caustics*, volume 50, pages 267–276. Banach Center Publications, 1999.
- [44] Dirk Siersma. Voronoi diagrams and Morse theory of the distance function. In *Geometry in Present Day Science*, pages 187–208. World Scientific, Singapore, 1999. Conference held at the University of Aarhus, Denmark, Jan. 1998.
- [45] R. C. Teixeira. *Curvature Motions, Medial Axes and Distance Transforms*. PhD thesis, Harvard University, Cambridge, MA, USA, June 1998.
- [46] V. A. Vassiliev. Homology of spaces of knots in any dimensions. *Philosophical Transactions: Mathematical, Physical and Engineering Sciences*, 359(1784):1343–1364, 2001.
- [47] J. A. Weickert. *Anisotropic Diffusion in Image Processing*. Teubner, Stuttgart, 1998.